European Journal of Medicinal Chemistry 45 (2010) 149–159

Contents lists available at ScienceDirect

European Journal of Medicinal Chemistry

journal homepage: http://www.elsevier.com/locate/ejmech

Original article

Synthesis, anticonvulsant activity and 3D-QSAR study of some prop-2-eneamido and 1-acetyl-pyrazolin derivatives of aminobenzothiazole

Nikhil D. Amnerkar, Kishore P. Bhusari*

Department of Medicinal Chemistry, Sharad Pawar College of Pharmacy, Rashtrasant Tukadoji Maharaj Nagpur University, Nagpur 441 110, Maharashtra, India

ARTICLE INFO

Article history:
Received 24 May 2009
Received in revised form
11 September 2009
Accepted 22 September 2009
Available online 30 September 2009

Keywords:
Aminobenzothiazole
Prop-2-eneamide
Pyrazoline
Anticonvulsant activity
3D-QSAR

ABSTRACT

A series of 6-substituted-[3-substituted-prop-2-eneamido]benzothiazole **9–32** and 6-substituted-2-[(1-acetyl-5-substituted)-2-pyrazolin-3-yl]aminobenzothiazole **33–56** were synthesized using appropriate synthetic route and evaluated experimentally against maximal electroshock test. Selected compounds were evaluated for neurotoxicity, hepatotoxicity and behavioral study. The most active compound, 6-methyl-2-[(1-acetyl-5-(4-chlorophenyl))-2-pyrazolin-3-yl]aminobenzothiazole **52** exhibited an ED_{50} of 25.49 μmol/kg, TD_{50} of 123.87 μmol/kg and high protective index (PI) of 4.86 compared to standard drug phenytoin. The 3D-QSAR analysis was carried out by PHASE program and a statistically reliable model with good predictive power ($r^2 = 0.9220$, $q^2 = 0.8144$) was achieved. The 3D-QSAR plots illustrated insights into the structure activity relationship of these compounds which may aids in the design of potent aminobenzothiazole derivatives as anticonvulsant agents.

1. Introduction

Epilepsy is a chronic neurological disorder characterized by the periodic and unpredictable occurrence of seizures that affects the people of all ages [1,2]. Being one of the world's oldest recognized disorders, it is surrounded by fear, discrimination, social and frightening manifestation [3]. A global campaign against epilepsy conducted by World Health Organization (WHO) in partnership with International Bureau for Epilepsy (IBE) and International League Against Epilepsy (ILAE) suggests that around 1% of world population at any time (about 50 million people worldwide) is afflicted with this neurological disorder. Every year about 2.4 million new cases are added to these figures [4,5]. Currently available antiepileptic drugs (AEDs) provide adequate seizure control in many patients, still about 28–30% of patients are estimated to be poorly treated [6,7]. Much efforts devoted in the recent years for the development of novel therapeutics resulted in the availability of several newer drugs (such as pregabalin, stiripentol, zonisamide, tiagabine, lamotrigine, levetiracetam, topiramate) as promising anticonvulsants [8–10]. These drugs have proven to be effective in reducing seizure, whilst their therapeutic efficacy is overcome by some undesirable side effects such as headache, nausea, hepatotoxicity, anorexia, ataxia, drowsiness, gastrointestinal disturbances and hirsutism [11,12]. These observations affirm the further scope and need for the development of newer agents.

Benzothiazole is among the usually occurred heterocyclic nuclei in many marine as well as natural plant products possessing the wide range of biological applications [13–17]. Recently, 2-aminobenzothiazoles emerged as new classes of anticonvulsant agents and one of its derivatives, riluzole is clinically available drug as anticonvulsant [18–23]. Moreover, pyrazoline ring is also an important building block in medicinal chemistry led to the discovery of a number of derivatives endowed with anticonvulsant, anti-inflammatory, antitubercular, antitumour and antidiabetic effects [24–28]. N–CO moiety is well recognized as pharmacophoric requirements in some of the well-known anticonvulsant agents with varied mechanism of action [6,29]. Previously, we have reported some [1,3]-oxazinane-2-thiones [18] and thioquinazoline [30] derivatives of 2-aminobenzothiazoles as moderately active anticonvulsant agents. These findings supported the significance of pyrazoline ring for anticonvulsant activity of 2-aminobenzothiazoles. In view of these and as a part of our enduring studies in the area of anticonvulsant agents it was thought of interest to combine the both pharmacophoric groups (pyrazoline ring and N–CO moiety). We have synthesized a series of 6-substituted-[3-substituted-prop-2-eneamido]benzothiazole **9–32**

* Corresponding author. Tel.: +91 7104 236352; fax: +91 7104 235084.
E-mail addresses: nikhilamnerkar@gmail.com (N.D. Amnerkar), kishore.bhusari@gmail.com (K.P. Bhusari).

0223-5234/$ – see front matter © 2009 Elsevier Masson SAS. All rights reserved.
doi:10.1016/j.ejmech.2009.09.037

and 6-substituted-2-[(1-acetyl-5-substituted)-2-pyrazolin-3-yl]aminobenzothiazole **33**–**56**, and evaluated for their potential as anticonvulsant agents.

The synthesized compounds and their anticonvulsant activity data were used to generate 3D-QSAR models in order to gain insights into the structural and molecular properties of these compounds using the PHASE [31,32] program (Schrödinger). In general, 3D-QSAR is a useful tool in molecular design and medicinal chemistry which allows the prediction of activity of structurally diverse compounds and also may assists in identifying new molecules with improved activity.

2. Chemistry

The synthesis of 6-substituted-[3-substituted-prop-2-eneamido]-benzothiazoles (compounds **9**–**32**) and 6-substituted-2-[(1-acetyl-5-substituted)-2-pyrazolin-3-yl]aminobenzothiazoles (compounds **33**–**56**) was accomplished as portrayed in Scheme 1. The compounds **5**–**8** were obtained by acetylation of compounds **1**–**4** with acetyl chloride following the methodology as described by A. Flohr et al. [33]. The aminobenzothiazole-chalcones (compounds **9**–**32**) were prepared by Claisen–Schmidt condensation of compounds **5**–**8** with appropriate aromatic aldehydes in ethanol and 10% NaOH at room temperature. Further, cyclization of chalcones (compounds **9**–**32**) in ethanolic hydrazine hydrate and glacial acetic acid yielded 6-substituted-2-[(1-acetyl-5-substituted)-2-pyrazolin-3-yl]aminobenzothiazole (compounds **33**–**56**). The structures of all the synthesized compounds were confirmed by spectral data (FTIR, ^{1}H NMR and EI-MS) and elemental analyses.

3. Pharmacology

All the synthesized compounds **9**–**32** and **33**–**56** were evaluated for their anticonvulsant activity against Maximal Electroshock (MES) induced seizures while the selected compounds were evaluated against subcutaneous pentylenetetrazole (scPTZ) induced seizure model in mice [18]. The minimal motor impairment was measured by the rotorod (neurotoxicity) test [20]. The test compounds were administered intraperitonealy at various dose levels ranging from 20–1000 μmol/kg body weight and the median effective dose (ED_{50}), median toxic dose (TD_{50}) and protection index (PI) values were determined. Selected compounds (**40**, **44**, **51**–**54** and **56**) with significant anticonvulsant activity were evaluated for the behavioral study using an actophotometer-scoring technique [34] and CNS study by determining the immobility time using Porsolt's swimpool test [35] with the standard drug carbamazepine, at the dose level of 100 μmol/kg. Compounds **52**, **53** and **56** were tested for hepatotoxic side effects using liver function tests [36].

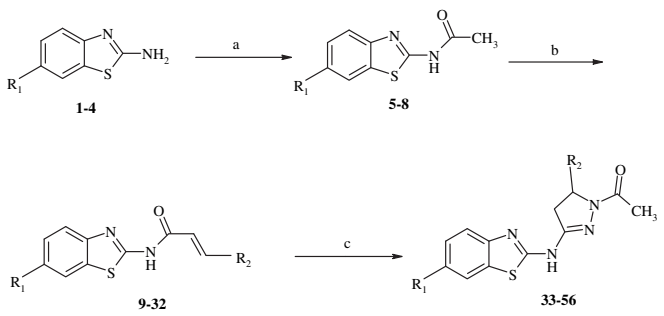

Scheme 1. General scheme for the synthesis of compounds **9**–**32** and **33**–**56**. Reagents and conditions: (a) $CHCl_3$, CH_3COCl, stir, 3 h, 0–5 °C; (b) dry EtOH, Ar–CHO, NaOH 10%, stir, 10–12 h, r.t.; (c) dry EtOH, $NH_2NH_2.H_2O$ 99%, CH_3COOH, reflux, 6–8 h.

4. Results and discussion

The present study describes the synthesis and anticonvulsant evaluation of some prop-2-eneamido and 1-acetyl-pyrazolin derivatives of aminobenzothiazole and development of 3D-QSARs using the generated data. A series of 48 new aminobenzothiazole derivatives (compounds **9**–**32** and **33**–**56**) were synthesized in satisfactory yields (52–80%) as illustrated in Scheme 1 and their structures were characterized by spectral data. The 6-substituted-[3-substituted-prop-2-eneamido]benzothiazole derivatives (compounds **9**–**32**) showed N–H and C═O stretching bands in the region of 3360–3298 and 1730–1690 cm^{-1}, respectively in their IR spectrum. While in their ^{1}H NMR spectra for these compounds exhibited two doublets for C–H in the regions of δ 6.48–6.89 ppm (CO–CH) and δ 7.14–7.42 ppm (CH–Ar) in addition to the singlet in the region δ 12.42–13.65 ppm (N–H). The IR spectrum of the 6-substituted-2-[(1-acetyl-5-substituted)-2-pyrazolin-3-yl]aminobenzothiazoles (compounds **33**–**56**) showed the stretching bands in the region of 1510–1470 cm^{-1} (N–N) and 1125–1085 cm^{-1} (C–N), respectively. In their ^{1}H NMR spectrum these derivatives exhibited the characteristic signals of H_A, H_B, H_X of pyrazoline ring as doublet of doublet in the regions δ 2.95–3.14, 3.32–3.95 and 5.06–5.85 ppm, respectively. However, all the other protons were resolved in appropriate regions confirming the assigned structures.

The result of anticonvulsant activity of the compounds **9**–**32** and **33**–**56** against MES induced seizures is depicted in Table 1. All of the compounds were active in the MES test which is an indicative of their ability to prevent seizure spread. Selected compounds **40**–**42**, **44**, **46**, **50**–**54** and **56** showed similar results when tested against scPTZ. In the neurological testing, none of these compounds demonstrated any sign of neurotoxicity. These compounds exhibited neurotoxicity (TD_{50}) at the maximum dose administered only after 0.5 h post-administration and the neurological deficit was found to be less compared to the standard drug, phenytoin. The protective index i.e. TD_{50}/ED_{50} showed significant results (Table 1). The most active compound **52** exhibited ED_{50} of 25.49 μmol/kg and a TD_{50} of 123.87 μmol/kg and high protective index (PI) of 4.86 compared to phenytoin. Compound **13** with the ED_{50} of 781.33 μmol/kg and TD_{50} 898.07 μmol/kg was the least effective and more toxic compound. The statistical analyses were carried out using one way ANOVA (Dunnet's test) at 95% confidence interval and all the activity data on comparison with vehicle control reaches the statistical significance ($p < 0.05$).

The behavioral activity of selected compounds **40**, **44**, **51**–**54** and **56** is summarized in Table 2. Compounds **44** and **52** along with phenytoin showed significant decrease in the locomotor activity, while the compound **56** did not showed any behavioral despair effect when compared with the control at $p < 0.05$ (Student's t test).

The effects of selected compounds **40**, **44**, **51**–**54** and **56** on duration of immobility time is presented as mean ± SEM using Porsolt's swimpool test (Table 3). No significant CNS depression was exhibited by compounds **44**, **52** and **53**, whilst the other compounds showed increase in immobility time compared with control at $p < 0.05$ and emerged as CNS depressants.

Selected compounds **52**, **53** and **56** were analyzed for their hepatotoxic side effects using liver function tests. The compounds were administered chronically to rats for 15 days at a dose of 100 μmol/kg. The enzyme serum glutamate oxaloacetate transaminase (SGOT) and serum glutamate pyruvate transaminase (SGPT) levels were estimated. All the tested compounds were safe since the serum level of these enzymes did not show any significant variation compared to the control (Table 4).

The anticonvulsant activity (ED_{50}) generated in the present studies for the series of 6-substituted-[3-substituted-prop-2-eneamido]benzothiazoles (compounds **9**–**32**) and 6-substituted-2-

Table 1
Anticonvulsant activity and neurotoxicity of compounds ($N = 6$)

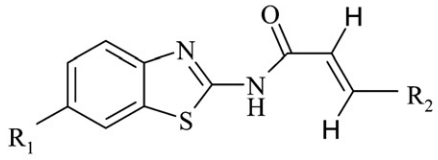

9–32

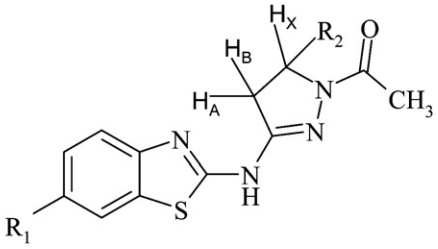

33–56

Compd	R_1	R_2	Intraperitoneal administration to mice			PI[d]	QSAR set[e]	pED_{50}[f]	
			MES[a]	scPTZ[b]	NT[c]			Actual	Pred[g]
9	H	C_6H_5	646	ND[h]	832	1.28	Training	3.19	3.21
33	H	C_6H_5	315	ND	498	1.57	Training	3.50	3.61
10	H	4-Cl-C_6H_5	367	ND	402	1.10	Test	3.44	3.33
34	H	4-Cl-C_6H_5	209	ND	364	1.73	Training	3.68	3.77
11	H	4-OH-C_6H_5	517	ND	925	1.78	Training	3.29	3.20
35	H	4-OH-C_6H_5	249	ND	513	2.06	Test	3.60	3.72
12	H	3-OH, 4-OMe-C_6H_5	495	ND	556	1.12	Test	3.31	3.21
36	H	3-OH, 4-OMe-C_6H_5	259	ND	382	1.47	Training	3.59	3.60
13	H	C_4H_3O	781	ND	898	1.15	Training	3.11	3.05
37	H	C_4H_3O	382	ND	538	1.41	Training	3.42	3.39
14	H	4-OMe-C_6H_5	435	ND	540	1.24	Test	3.36	3.29
38	H	4-OMe-C_6H_5	226	ND	369	1.63	Test	3.65	3.54
15	Cl	C_6H_5	425	ND	570	1.34	Training	3.37	3.48
39	Cl	C_6H_5	161	ND	245	1.52	Test	3.79	3.89
16	Cl	4-Cl-C_6H_5	204	ND	576	2.82	Test	3.69	3.73
40	Cl	4-Cl-C_6H_5	79.47	81.52	345	4.35	Training	4.10	3.94
17	Cl	4-OH-C_6H_5	322	ND	413	1.28	Training	3.49	3.52
41	Cl	4-OH-C_6H_5	106	107.35	210	1.97	Test	3.97	4.16
18	Cl	3-OH, 4-OMe-C_6H_5	320	ND	470	1.46	Test	3.51	3.66
42	Cl	3-OH, 4-OMe-C_6H_5	127	132.48	276	2.16	Test	3.89	3.94
19	Cl	C_4H_3O	544	ND	658	1.20	Training	3.26	3.38
43	Cl	C_4H_3O	212	ND	387	1.82	Training	3.67	3.72
20	Cl	4-OMe-C_6H_5	259	ND	465	1.79	Training	3.59	3.69
44	Cl	4-OMe-C_6H_5	93.29	97.32	187	2.01	Test	4.03	3.89
21	NO_2	C_6H_5	485	ND	633	1.30	Training	3.31	3.36
45	NO_2	C_6H_5	216	ND	357	1.65	Training	3.67	3.75
22	NO_2	4-Cl-C_6H_5	259	ND	787	3.03	Training	3.59	3.47
46	NO_2	4-Cl-C_6H_5	132	137.65	328	2.48	Training	3.88	3.76
23	NO_2	4-OH-C_6H_5	382	ND	602	1.57	Training	3.42	3.34
47	NO_2	4-OH-C_6H_5	162	ND	210	1.29	Training	3.79	3.88
24	NO_2	3-OH, 4-OMe-C_6H_5	372	ND	793	2.13	Training	3.43	3.30
48	NO_2	3-OH, 4-OMe-C_6H_5	178	ND	256	1.43	Training	3.75	3.65
25	NO_2	C_4H_3O	597	ND	834	1.39	Test	3.22	3.15
49	NO_2	C_4H_3O	274	ND	355	1.29	Training	3.56	3.52
26	NO_2	4-OMe-C_6H_5	315	ND	466	1.47	Training	3.50	3.42
50	NO_2	4-OMe-C_6H_5	145	149.08	246	1.69	Test	3.84	3.71
27	CH_3	C_6H_5	380	ND	534	1.40	Test	3.42	3.58
51	CH_3	C_6H_5	106	111.57	265	2.49	Training	3.97	4.00
28	CH_3	4-Cl-C_6H_5	152	ND	408	2.67	Training	3.82	3.78
52	CH_3	4-Cl-C_6H_5	25.46	27.46	123	4.86	Test	4.59	4.22
29	CH_3	4-OH-C_6H_5	271	ND	387	1.42	Test	3.57	3.68
53	CH_3	4-OH-C_6H_5	50.21	54.31	157	3.14	Training	4.30	4.14
30	CH_3	3-OH, 4-OMe-C_6H_5	271	ND	321	1.18	Test	3.57	3.60
54	CH_3	3-OH, 4-OMe-C_6H_5	73.91	75.64	147	1.99	Training	4.13	4.01
31	CH_3	C_4H_3O	505	ND	603	1.19	Test	3.30	3.35
55	CH_3	C_4H_3O	160	ND	243	1.51	Training	3.79	3.84
32	CH_3	4-OMe-C_6H_5	209	ND	468	2.24	Test	3.68	3.60
56	CH_3	4-OMe-C_6H_5	37.32	39.44	174	4.68	Training	4.43	4.35
Phenytoin			13.78	–	110	8.01	–	–	–

[a] All compounds were administered by ip injection at doses of 20–1000 μmol/kg and values were determined at $t = 0.5$ h. MES indicates maximum electroshock test and the data are represented in terms of ED_{50}.
[b] Subcutaneous pentylenetetrazole test.
[c] Neurotoxicity screening using rotorod test and values are expressed in terms of TD_{50}.
[d] Protection index ($PI = TD_{50}/ED_{50}$).
[e] It represents the training set (29 compound) and test set (19 compound).
[f] Biological activity expressed as $pED_{50} = -\log(ED_{50} \times 10^{-6})$] and used for 3D-QSAR studies.
[g] Predicted activity from PHASE 3D-QSAR program.
[h] ND: activity not determined.

Table 2
Behavioral activity of the selected compounds ($N = 6$).

Compd	Activity score using actophotometer		% Change in locomotor activity[b]
	Control (24 h before) '*X*'	Post-treatment[a] (0.5 h after) '*Y*'	
40	120 ± 2.7	82 ± 1.6	31.66 (↓)
44	142 ± 3.4	91 ± 2.1	35.91 (↓)
51	188 ± 4.2	143 ± 1.1	23.93 (↓)
52	160 ± 1.3	103 ± 1.4	35.62 (↓)
53	148 ± 0.9	117 ± 0.8	20.94 (↓)
54	122 ± 3.2	86 ± 1.7	29.50 (↓)
56	144 ± 1.6	141 ± 2.5 NS	2.08 (↓)
Phenytoin	167 ± 2.2	98 ± 1.3	41.31 (↓)

[a] Each value represents the mean ± SEM significantly different from the control at $p < 0.05$, NS denotes not significant at $p < 0.05$ (Student's *t* test), locomotor activity score was measured for 10 min.
[b] % Change is calculated as 100−[(*Y*x100)/*X*].

[(1-acetyl-5-substituted)-2-pyrazolin-3-yl]aminobenzothiazoles (compounds **33**–**56**) was employed for the generation of 3D-QSAR models with the aim that these models could provide useful pharmacophoric information for the future efforts in the development of more potent molecules in these series of chemical classes. The statistically significant 3D-QSAR models were generated using 29 molecules as the training set and was validated using test set (19 compounds) (Table 1) employing PHASE, the pharmacophore modeling tool [37]. Using PHASE, one can exhaustively identify the spatial arrangements of functional groups that are common and essential for the biological activity of the ligands under investigation [38,39].

In general, the total of 101 five point hypotheses were obtained upon the completion of scoring process and the top four high ranking pharmacophore hypotheses were analyzed. The statistical and partial least square (PLS) analyses results for four of the top ranking pharmacophores (model 1–4) are summarized in Table 5. The model 1 was consisting of two hydrogen-bond acceptor, one positive group and two aromatic rings. Model 2 was composed of two hydrogen-bond acceptor and three aromatic rings. The model 3 consisted of three hydrogen-bond acceptors and two aromatic rings while model 4 possessed one hydrogen-bond acceptor, one positive group and three aromatic rings. The model 1 exhibited comparatively better PLS statistical qualities and excellent prediction of the external test set molecules, therefore was considered for explaining the SAR of the molecules under investigations. Model 1 showed conventional correlation coefficient (r^2) of 0.9220 with four components, test set prediction (q^2) of 0.8144 and Pearson-R (r_p) of 0.9114. The high value of variance ratio (*F*) observed for this model indicates its statistical robustness which is further supported by significance level of variance ratio (*P*). The value of $P < 0.05$ indicates greater degree of confidence means *F* is significant at the 95% level. The low standard deviation (SD) and root-mean-squared error (RMSE) contributes significantly to the model. Fig. 1 shows the graph of actual versus predicted activities for training and test set molecules using this model.

Table 3
Effect of selected compounds on duration of immobility time in Porsolt's swimpool test.

Compd	Mean average immobility time (s)[a]	
	Control (24 before)	Post-treatment (0.5 h after)
40	92 ± 1.2	134 ± 2.4
44	82 ± 2.9	88 ± 1.7 NS
51	104 ± 1.8	151 ± 3.6
52	87 ± 1.5	91 ± 0.8 NS
53	128 ± 2.4	136 ± 1.6
54	113 ± 3.1	177 ± 3.2
56	97 ± 2.2	163 ± 2.4
Carbamazepine	78 ± 0.9	145 ± 1.4

[a] Each value represents the mean ± SEM of six rats significantly different from the control at $p < 0.05$, NS denotes not significant at $p < 0.05$ (Student's *t* test).

Table 4
SGOT and SGPT estimation of selected compounds in serum level.

Compd	SGOT[a] (units/ml)	SGPT[b] (units/ml)
Control	92.2 ± 2.78	35.4 ± 2.68
52	93.3 ± 3.13	33.1 ± 1.62
53	89.6 ± 1.17	30.2 ± 2.51
56	95.4 ± 1.74	38.4 ± 1.83
phenytoin	101.5 ± 5.13	41.3 ± 2.18

[a] Each value represents the mean ± SEM of six rats, not significant from the control value at $p < 0.05$ (Student's *t* test).
[b] Control group (six rats) were treated with 0.5% methyl cellulose for 15 days.

The common pharmacophore generated from the best PHASE hypothesis with aligned compound **52** is shown in Fig. 2. It showed pharmacophoric features as red sphere for hydrogen-bond acceptor (A) with the arrows pointing in the direction of lone pair, blue sphere for positively charged group (P) and orange torus for aromatic rings (R). In addition, the 3D-QSAR results are also visualized as 3D plots of crucial pharmacophore regions in which the blue cubes indicate increase and red cubes (regions) indicate decrease in activity for specific feature in the ligand regions. Fig. 3 a–e shows the 3D-QSAR plots with specific features relating to most active conformer overlaid with the best-generated pharmacophore hypothesis (compound **52**) and their relation with the biological activity of molecules.

In the electron withdrawing (includes hydrogen-bond acceptor) plot (Fig. 3a), the blue regions at 3-nitrogen and 2-NH position of benzothiazole ring, in the vicinity of N-CO moiety and 4′ position of 5-phenyl ring favors the activity (compounds **34**, **40**, **46** and **52**), while electron withdrawing unfavorable red region surrounding 6 position of benzothiazole ring reduces the activity (compounds **39** and **43**). In the hydrogen-bond donor plots, the blue regions at 6- and 2-NH position of benzothiazole ring show the significance of proton in the hydrogen bond formation with the receptor surface (compounds **53**, **54** and **56**). The red regions in the vicinity of 3′ and 4′ position of 5-phenyl ring suggested that the substructure fragments with hydrogen-bond donor in this area may reduce the activity (compounds **36**, **42** and **48**, Fig. 3b). In the negative ionic plots (Fig. 3c), blue regions at 4′ position of 5-phenyl ring suggests that increased activity may be anticipated by moderate negatively charged substituents at 4′ position (compounds **34** and **52**), whereas red region surrounding the 6 position of benzothiazole ring disfavors the activity (compounds **40** and **46**). In addition, the

Table 5
Summary of PHASE 3D-QSAR statistical results.

Pharmacophore	Model 1	Model 2	Model 3	Model 4
Hypotheses	AAPRR	AARRR	AAARR	APRRR
PLS statistics of QSAR model				
r^2	0.9220	0.9128	0.9011	0.9052
SD	0.0585	0.0682	0.0843	0.0781
F	82.4	76.2	61.3	64.5
P	$1.51e^{-13}$	$4.22e^{-12}$	$3.43e^{-11}$	$6.46e^{-12}$
Number of PLS factor	4	4	4	4
External test set prediction				
q^2	0.8144	0.8112	0.8021	0.8078
r_p	0.9114	0.9105	0.9068	0.9024
RMSE	0.1385	0.1346	0.1312	0.1363

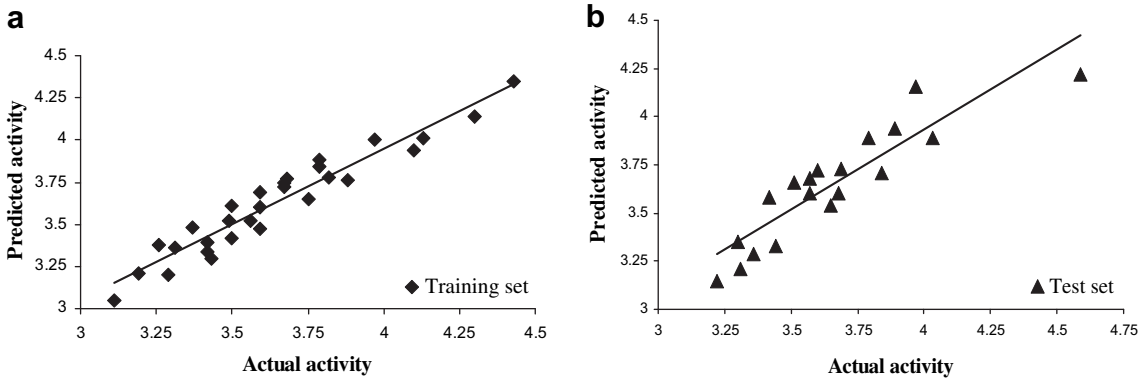

Fig. 1. Plots of predicted versus actual activity values for the training set (a) and test set (b) molecules based on PHASE 3D-QSAR model.

positive ionic favorable blue region (Fig. 3d) observed at 6 position of benzothiazole and near tertiary nitrogen of pyrazoline ring defines that an increase in positive group may result in enhanced activity (compound **33**). These regions include partial positive charges associated with hydrogen atoms bound to carbon, which can be correlated with lipophilic interactions. The red region was observed at 4′ position of 5-phenyl ring which results in reduced activity (compounds **33** and **38**). The hydrophobic (nonpolar) plot indicates desired/undesired hydrophobic regions around two phenyl rings (Fig. 3e). The blue region observed in the vicinity of $NCOCH_3$ group and 6 position of benzothiazole ring signifies that substitution with hydrophobic group may result in enhanced activity (compounds **35** and **53**); whereas a slight variation in the phenyl ring results in decreased activity (compound **55**). The disfavored red region in the vicinity of 4′ position of 5-phenyl ring suggests that hydrophobic group in this area resulted in decreased activity (compounds **53** and **56**).

Additionally, the compounds **9**–**32** displayed weaker anticonvulsant activity which might be due to the lack of positive group (tertiary ring nitrogen) which is a part of best pharmacophore model and variation in the position of N-CO moiety. From these findings, one can assumed 1-acetyl-pyrazolin ring as a crucial pharmacophoric group for the anticonvulsant activity of benzothiazoles.

5. Conclusions

In the present studies, a series of 6-substituted-[3-substituted-prop-2-eneamido]benzothiazole **9**–**32** and 6-substituted-2-[(1-acetyl-5-substituted)-2-pyrazolin-3-yl]aminobenzothiazole **33**–**56** were synthesized successfully in convenient steps in 52–80% yields. All compounds were tested for anticonvulsant activity to determine ED_{50} values and the activity data was supported by CNS depressant and hepatotoxicity studies. Although the most active in derivatives in these series (compound **52**) showed relatively less activity than the phenytoin which can be overruled as the activities of compound **52** was statistically significant and can be used as a lead for further development of more potent anticonvulsant agents. In view of this and our ongoing efforts to develop anticonvulsant agents, it was thought of interest to study the SAR quantitatively using these series of molecules although the substituents are not so diverse but they are varying significantly in the 3D space. The statistically significant 3D-QSAR model with r^2 of 0.9220 and q^2 of 0.8144 was developed using PHASE and analyzed in order to understand the trends of these molecules for their anticonvulsant properties. The influence of electron withdrawing, hydrogen-bond donor, negative/positive ionic and hydrophobic groups was analyzed and discussed using the 3D-QSAR PHASE hypotheses. We believe that the derived 3D-QSAR as well as clues for possible structural modifications will be of interest and significance for the strategic design of more potent molecules in the benzothiazoles as anticonvulsant agents.

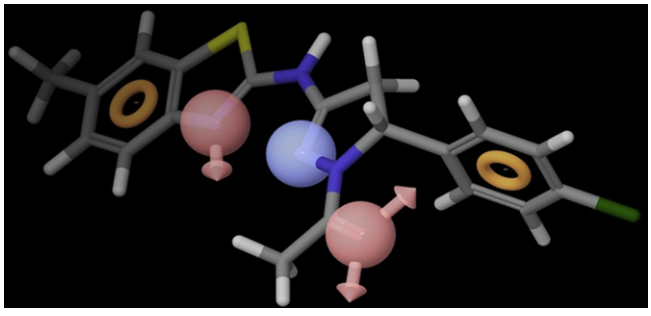

Fig. 2. Common pharmacophore generated from the best PHASE hypothesis. Pharmacophore features are red sphere for hydrogen-bond acceptors (A) with the arrows pointing in the direction of lone pair, blue sphere for positively charged group (P) and orange torus for aromatic rings (R). Compound 52 aligned to the pharmacophore for which blue indicates nitrogen, yellow refers to sulphur, green for chlorine, gray indicates carbon and white refers to hydrogen.

6. Experimental protocols

6.1. Instrumentation and chemicals

All the chemicals and solvents employed in the synthesis were supplied by Merck (Germany), Fluka (Germany) and SD Fine chemicals (India) and used without purification. Melting point were determined on a digital melting point apparatus Electrothermal 1A 9200 (U.K.) and are uncorrected. All the reactions were monitored by TLC performed on 2.0–6.0 cm aluminium sheets precoated with silica gel 60 (HF-254, E. Merck, India). The IR spectra were recorded on a Shimadzu FTIR 8400S spectrophotometer (Kyto, Japan) using KBr optics. ^1H NMR spectra were recorded in $CDCl_3$ on a Varian Mercury YH-300 MHz spectrophotometer (Palo Alto, CA, USA) and chemical shifts (δ) are given in ppm relative to TMS. Mass spectra were recorded at 70 eV on Jeol D-300 spectrometer (Tokyo, Japan). Elemental analyses were carried out using FLASH EA 1112 CHN analyzer (Thermo Finnigan, Italy) and found within ±0.4% of theoretical values.

6.2. Syntheses

6.2.1. General synthesis of 6-substituted-[3-substituted-prop-2-eneamido]-benzothiazole (**9**–**32**)

To a solution of 6-substituted-2-acetamidobenzothiazole (0.01 mol) in dry ethanol (50 ml), appropriate aldehydes (0.01 mol)

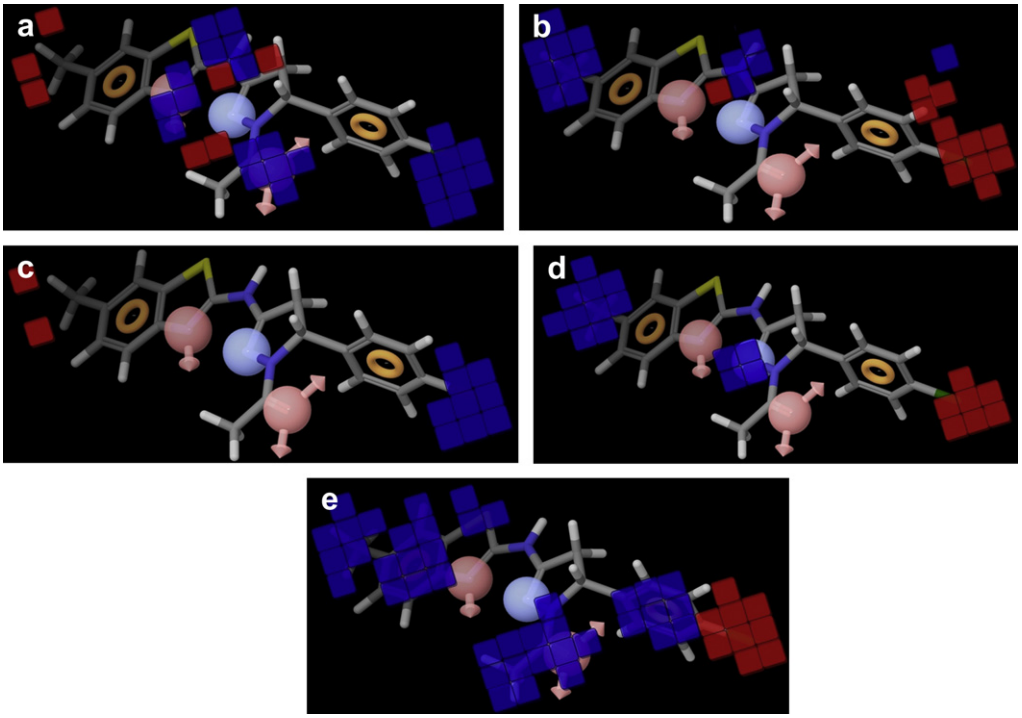

Fig. 3. (a–e) PHASE 3D plots of crucial pharmacophore region based on model 1 displayed with compound 52. Positive coefficient favored areas (contributing for increase in activity) are represented by blue cubes. Negative coefficient favored areas (contributing for decrease in activity) are represented by red cubes. (**3a**) Hydrogen-bond acceptor; (**3b**) Hydrogen-bond donor; (**3c**) Negative-ionic groups; (**3d**) Positive-ionic groups; (**3e**) Hydrophobic region.

were added in the presence of NaOH solution (5 ml, 10%). The reaction mixture was stirred at room temperature for 10–12 h. The excess solvent was distilled off in vacuum. The remaining mixture was poured onto ice–water, filtered and washed with water. The residue was dried and purified by recrystallization from ethanol (70%) to obtain 6-substituted-[3-substituted-prop-2-eneamido]-benzothiazoles **9**–**32**.

*6.2.1.1. 3-Phenyl-prop-2-eneamidobenzothiazole (**9**).* White crystals; Yield: 79%; mp 149–151 °C; R_f 0.78 (ethyl acetate); IR (KBr, cm^{-1}): 3320 (NH), 1710 (C═O), 1540 (C═N); ^1H NMR ($CDCl_3$): δ 6.85 (d, $J = 7.6$ Hz, 1H, CO–CH), 7.42 (d, $J = 6.8$ Hz, 1H, CH–Ar), 7.58–8.14 (m, 9H, Ar–H), 13.58 (s, 1H, NH); EI-MS: m/z $[M + H]^+$ 281; Anal. Calcd for $C_{16}H_{12}N_2OS$: C, 68.55; H, 4.31; N, 9.99; S, 11.44. Found: C, 68.53; H, 4.33; N, 9.98; S, 11.46.

*6.2.1.2. 3-(4-Chlorophenyl)-prop-2-eneamidobenzothiazole (**10**).* White crystals; Yield: 73%; mp 162–164 °C; R_f 0.62 (ethyl acetate); IR (KBr, cm^{-1}): 3330 (NH), 1720 (C═O), 1550 (C═N); ^1H NMR ($CDCl_3$): δ 6.86 (d, $J = 7.8$ Hz, 1H, CO–CH), 7.43 (d, $J = 6.8$ Hz, 1H, CH–Ar), 7.62–8.22 (m, 8H, Ar–H), 13.62 (s, 1H, NH); EI-MS: m/z $[M + H]^+$ 315; Anal. Calcd for $C_{16}H_{11}ClN_2OS$: C, 61.05; H, 3.52; N, 8.90; S, 10.19. Found: C, 61.06; H, 3.53; N, 8.89; S, 10.20.

*6.2.1.3. 3-(4-Hydroxyphenyl)-prop-2-eneamidobenzothiazole (**11**).* Pale white crystals; Yield: 59%; mp 261–262 °C; R_f 0.61 (ethyl acetate); IR (KBr, cm^{-1}): 3485 (OH), 3350 (NH), 1710 (C═O), 1560 (C═N); ^1H NMR ($CDCl_3$): δ 6.88 (d, $J = 8.3$ Hz, 1H, CO–CH), 7.39 (d, $J = 6.6$ Hz, 1H, CH–Ar), 7.61–8.09 (m, 8H, Ar–H), 9.44 (s, 1H, OH), 13.64 (s, 1H, NH); EI-MS: m/z $[M + H]^+$ 297; Anal. Calcd for $C_{16}H_{12}N_2O_2S$: C, 64.85; H, 4.09; N, 9.45; S, 10.82. Found: C, 64.84; H, 4.10; N, 9.44; S, 10.83.

*6.2.1.4. 3-(3-Hydroxy-4-methoxyphenyl)-prop-2-eneamidobenzothiazole (**12**).* Muddy white crystals; Yield: 64%; mp 218–220 °C; R_f 0.58 (ethyl acetate); IR (KBr, cm^{-1}): 3620 (OH), 3330 (NH), 1700 (C═O), 1530 (C═N); ^1H NMR ($CDCl_3$): δ 3.83 (s, 3H, OCH_3), 6.88 (d, $J = 7.9$ Hz, 1H, CO–CH), 7.35 (d, $J = 6.5$ Hz, 1H, CH–Ar), 7.62–8.14 (m, 7H, Ar–H), 9.46 (s, 1H, OH), 13.58 (s, 1H, NH); EI-MS: m/z $[M + H]^+$ 327; Anal. Calcd for $C_{17}H_{14}N_2O_3S$: C, 62.56; H, 4.32; N, 8.58; S, 9.82. Found: C, 62.55; H, 4.33; N, 8.57; S, 9.84.

*6.2.1.5. 3-(Furan-2-yl)-prop-2-eneamidobenzothiazole (**13**).* Reddish-brown crystals; Yield: 59%; mp 186–188 °C; R_f 0.51 (ethyl acetate); IR (KBr, cm^{-1}): 3350 (NH), 1710 (C═O), 1540 (C═N); ^1H NMR ($CDCl_3$): δ 6.87 (d, $J = 8.1$ Hz, 1H, CO–CH), 7.38 (d, $J = 6.9$ Hz, 1H, CH–Ar), 7.74–8.21 (m, 7H, Ar–H), 13.61 (s, 1H, NH); EI-MS: m/z $[M + H]^+$ 271; Anal. Calcd for $C_{14}H_{10}N_2O_2S$: C, 62.21; H, 3.73; N, 10.36; S, 11.86. Found: C, 62.22; H, 3.72; N, 10.37; S, 11.84.

*6.2.1.6. 3-(4-Methoxyphenyl)-prop-2-eneamidobenzothiazole (**14**).* White crystals; Yield: 52%; mp 243–245 °C; R_f 0.74 (ethyl acetate); IR (KBr, cm^{-1}): 3340 (NH), 1690 (C═O), 1550 (C═N); ^1H NMR ($CDCl_3$): δ 3.79 (s, 3H, OCH_3), 6.87 (d, $J = 8.3$ Hz, 1H, CO–CH), 7.37 (d, $J = 7.2$ Hz, 1H, CH–Ar), 7.53–8.18 (m, 8H, Ar–H), 13.63 (s, 1H, NH); EI-MS: m/z $[M + H]^+$ 280; Anal. Calcd for $C_{16}H_{11}N_2OS$: C, 68.80; H, 3.97; N, 10.03; S, 11.48. Found: C, 68.81; H, 3.97; N, 10.05; S, 11.46.

*6.2.1.7. 6-Chloro-[3-phenyl-prop-2-eneamido]benzothiazole (**15**).* Pale yellow crystals; Yield: 65%; mp 166–168 °C; R_f 0.64 (ethyl acetate); IR (KBr, cm^{-1}): 3360 (NH), 1710 (C═O), 1530 (C═N); ^1H NMR ($CDCl_3$): δ 6.89 (d, $J = 7.8$ Hz, 1H, CO–CH), 7.37 (d, $J = 6.9$ Hz, 1H, CH–Ar), 7.56–8.13 (m, 8H, Ar–H), 13.62 (s, 1H, NH); EI-MS: m/z $[M + H]^+$ 316; Anal. Calcd for $C_{16}H_{11}ClN_2OS$: C, 61.05; H, 3.52; N, 8.90; S, 10.19. Found: C, 61.07; H, 3.52; N, 8.89; S, 10.20.

*6.2.1.8. 6-Chloro-[3-(4-chlorophenyl)-prop-2-eneamido]benzothiazole (**16**).* White-creamish crystals; Yield: 61%; mp 188–190 °C; R_f 0.62 (ethyl acetate); IR (KBr, cm^{-1}): 3350 (NH), 1700 (C═O), 1540

(C=N); ^{1}H NMR ($CDCl_3$): δ 6.87 (d, J = 8.1 Hz, 1H, CO–CH), 7.35 (d, J = 7.2 Hz, 1H, CH–Ar), 7.57–8.18 (m, 7H, Ar–H), 13.63 (s, 1H, NH); EI-MS: m/z $[M+H]^+$ 350; Anal. Calcd for $C_{16}H_{10}Cl_2N_2OS$: C, 55.03; H, 2.89; N, 8.02; S, 9.18. Found: C, 55.05; H, 2.88; N, 8.03; S, 9.17.

*6.2.1.9. 6-Chloro-[3-(4-hydroxyphenyl)-prop-2-eneamido]benzothiazole (**17**).* Pale brown crystals; Yield: 69%; mp 262–264 °C; R_f 0.57 (ethyl acetate); IR (KBr, cm^{-1}): 3555 (OH), 3340 (NH), 1700 (C=O), 1545 (C=N); ^{1}H NMR ($CDCl_3$): δ 6.88 (d, J = 8.5 Hz, 1H, CO–CH), 7.34 (d, J = 7.3 Hz, 1H, CH–Ar), 7.49–8.13 (m, 7H, Ar–H), 9.44 (s, 1H, OH), 13.62 (s, 1H, NH); EI-MS: m/z $[M+H]^+$ 331; Anal. Calcd for $C_{16}H_{11}ClN_2O_2S$: C, 58.09; H, 3.35; N, 8.47; S, 9.69. Found: C, 58.08; H, 3.36; N, 8.48; S, 9.68.

*6.2.1.10. 6-Chloro-[3-(3-hydroxy-4-methoxyphenyl)-prop-2-eneamido]benzothiazole (**18**).* Muddy crystalline solid; Yield: 58%; mp 217–219 °C; R_f 0.54 (ethyl acetate); IR (KBr, cm^{-1}): 3520 (OH), 3340 (NH), 1710 (C=O), 1530 (C=N); ^{1}H NMR ($CDCl_3$): δ 3.83 (s, 3H, OCH_3), 6.86 (d, J = 8.3 Hz, 1H, CO–CH), 7.38 (d, J = 7.1 Hz, 1H, CH–Ar), 7.53–8.18 (m, 6H, Ar–H), 9.46 (s, 1H, OH), 13.65 (s, 1H, NH); EI-MS: m/z $[M+H]^+$ 362; Anal. Calcd for $C_{17}H_{13}ClN_2O_3S$: C, 56.59; H, 3.63; N, 7.76; S, 8.89. Found: C, 56.58; H, 3.62; N, 7.75; S, 8.90.

*6.2.1.11. 6-Chloro-[3-(furan-2-yl)-prop-2-eneamido]benzothiazole (**19**).* Yellowish-brown solid; Yield: 67%; mp 238–240 °C; R_f 0.48 (ethyl acetate); IR (KBr, cm^{-1}): 3350 (NH), 1730 (C=O), 1560 (C=N); ^{1}H NMR ($CDCl_3$): δ 6.78 (d, J = 8.2 Hz, 1H, CO–CH), 7.42 (d, J = 6.8 Hz, 1H, CH–Ar), 7.68–8.23 (m, 6H, Ar–H), 13.13 (s, 1H, NH); EI-MS: m/z $[M+H]^+$ 306; Anal. Calcd for $C_{14}H_9ClN_2O_2S$: C, 55.18; H, 2.98; N, 9.19; S, 10.52. Found: C, 55.20; H, 2.98; N, 9.18; S, 10.51.

*6.2.1.12. 6-Chloro-[3-(4-methoxyphenyl)-prop-2-eneamido]benzothiazole (**20**).* Pale yellow crystals; Yield: 62%; mp 243–245 °C; R_f 0.62 (ethyl acetate); IR (KBr, cm^{-1}): 3350 (NH), 1690 (C=O), 1540 (C=N); ^{1}H NMR ($CDCl_3$): δ 3.81 (s, 3H, OCH_3), 6.87 (d, J = 7.8 Hz, 1H, CO–CH), 7.37 (d, J = 6.7 Hz, 1H, CH–Ar), 7.51–8.16 (m, 7H, Ar–H), 13.64 (s, 1H, NH); EI-MS: m/z $[M+H]^+$ 346; Anal. Calcd for $C_{17}H_{13}ClN_2O_2S$: C, 59.21; H, 3.80; N, 8.12; S, 9.30. Found: C, 59.22; H, 3.81; N, 8.11; S, 9.31.

*6.2.1.13. 6-Nitro-[3-phenyl-prop-2-eneamido]benzothiazole (**21**).* Yellow solid; Yield: 52%; mp 263–265 °C; R_f 0.48 (ethyl acetate); IR (KBr, cm^{-1}): 3307 (NH), 1695 (C=O), 1569 (C=N); ^{1}H NMR ($CDCl_3$): δ 6.75 (d, J = 8.2 Hz, 1H, CO–CH), 7.34 (d, J = 6.8 Hz, 1H, CH–Ar), 7.65–8.14 (m, 8H, Ar–H), 12.86 (s, 1H, NH); EI-MS: m/z $[M+H]^+$ 327; Anal. Calcd for $C_{16}H_{11}N_3O_3S$: C, 59.07; H, 3.41; N, 12.92; S, 9.86. Found: C, 59.08; H, 3.40; N, 12.93; S, 9.87.

*6.2.1.14. 6-Nitro-[3-(4-chlorophenyl)-prop-2-eneamido]benzothiazole (**22**).* Yellow solid; Yield: 63%; mp 241–243 °C; R_f 0.51 (ethyl acetate); IR (KBr, cm^{-1}): 3324 (NH), 1704 (C=O), 1553 (C=N); ^{1}H NMR ($CDCl_3$): δ 6.62 (d, J = 7.9 Hz, 1H, CO–CH), 7.21 (d, J = 6.7 Hz, 1H, CH–Ar), 7.72–8.27 (m, 7H, Ar–H), 12.72 (s, 1H, NH); EI-MS: m/z $[M+H]^+$ 361; Anal. Calcd for $C_{16}H_{10}ClN_3O_3S$: C, 53.41; H, 2.80; N, 11.68; S, 8.91. Found: C, 53.43; H, 2.81; N, 11.67; S, 8.90.

*6.2.1.15. 6-Nitro-[3-(4-hydroxyphenyl)-prop-2-eneamido]benzothiazole (**23**).* Yellow solid; Yield: 58%; mp 207–209 °C; R_f 0.62 (ethyl acetate); IR (KBr, cm^{-1}): 3610 (OH), 3308 (NH), 1723 (C=O), 1542 (C=N); ^{1}H NMR ($CDCl_3$): δ 6.48 (d, J = 8.3 Hz, 1H, CO–CH), 7.36 (d, J = 7.1 Hz, 1H, CH–Ar), 7.68–8.12 (m, 7H, Ar–H), 9.71 (s, 1H, OH), 12.88 (s, 1H, NH); EI-MS: m/z $[M+H]^+$ 343; Anal. Calcd for $C_{16}H_{11}N_3O_4S$: C, 56.30; H, 3.25; N, 12.31; S, 9.39. Found: C, 56.32; H, 3.26; N, 12.30; S, 9.38.

*6.2.1.16. 6-Nitro-[3-(3-hydroxy-4-methoxyphenyl)-prop-2-eneamido]-benzothiazole (**24**).* Yellow solid; Yield: 71%; mp 186–188 °C; R_f 0.68 (ethyl acetate); IR (KBr, cm^{-1}): 3540 (OH), 3345 (NH), 1723 (C=O), 1568 (C=N); ^{1}H NMR ($CDCl_3$): δ 3.88 (s, 3H, OCH_3), 6.58 (d, J = 7.9 Hz, 1H, CO–CH), 7.22 (d, J = 6.7 Hz, 1H, CH–Ar), 7.66–8.12 (m, 7H, Ar–H), 9.87 (s, 1H, OH), 12.74 (s, 1H, NH); EI-MS: m/z $[M+H]^+$ 373; Anal. Calcd for $C_{17}H_{13}N_3O_5S$: C, 54.98; H, 3.53; N, 11.31; S, 8.64. Found: C, 54.97; H, 3.53; N, 11.30; S, 8.64.

*6.2.1.17. 6-Nitro-[3-(furan-2-yl)-prop-2-eneamido]benzothiazole (**25**).* Yellow solid; Yield: 52%; mp 220–222 °C; R_f 0.53 (ethyl acetate); IR (KBr, cm^{-1}): 3298 (NH), 1708 (C=O), 1547 (C=N); ^{1}H NMR ($CDCl_3$): δ 6.83 (d, J = 8.1 Hz, 1H, CO–CH), 7.36 (d, J = 7.2 Hz, 1H, CH–Ar), 7.72–8.38 (m, 6H, Ar–H), 13.08 (s, 1H, NH); EI-MS: m/z $[M+H]^+$ 317; Anal. Calcd for $C_{14}H_9N_3O_4S$: C, 53.33; H, 2.88; N, 13.33; S, 10.17. Found: C, 53.31; H, 2.87; N, 13.35; S, 10.19.

*6.2.1.18. 6-Nitro-[3-(4-methoxyphenyl)-prop-2-eneamido]benzothiazole (**26**).* Yellow solid; Yield: 64%; mp 192–194 °C; R_f 0.66 (ethyl acetate); IR (KBr, cm^{-1}): 3322 (NH), 1714 (C=O), 1556 (C=N); ^{1}H NMR ($CDCl_3$): δ 3.83 (s, 3H, OCH_3), 6.64 (d, J = 8.1 Hz, 1H, CO–CH), 7.14 (d, J = 6.9 Hz, 1H, CH–Ar), 7.58–8.04 (m, 7H, Ar–H), 12.42 (s, 1H, NH); EI-MS: m/z $[M+H]^+$ 357; Anal. Calcd for $C_{17}H_{13}N_3O_4S$: C, 57.46; H, 3.69; N, 11.82; S, 9.02. Found: C, 57.44; H, 3.68; N, 11.83; S, 9.03.

*6.2.1.19. 6-Methyl-[3-phenyl-prop-2-eneamido]benzothiazole (**27**).* Pale brown crystals; Yield: 73%; mp 177–179 °C; R_f 0.55 (ethyl acetate); IR (KBr, cm^{-1}): 3318 (NH), 1694 (C=O), 1572 (C=N); ^{1}H NMR ($CDCl_3$): δ 2.48 (s, 3H, Ar–CH_3), 6.48 (d, J = 8.1 Hz, 1H, CO–CH), 7.23 (d, J = 6.5 Hz, 1H, CH–Ar), 7.61–8.35 (m, 8H, Ar–H), 12.73 (s, 1H, NH); EI-MS: m/z $[M+H]^+$ 296; Anal. Calcd for $C_{17}H_{14}N_2OS$: C, 69.36; H, 4.79; N, 9.52; S, 10.89. Found: C, 69.37; H, 4.77; N, 9.53; S, 10.88.

*6.2.1.20. 6-Methyl-[3-(4-chlorophenyl)-prop-2-eneamido]benzothiazole (**28**).* Pale orange solid; Yield: 78%; mp 188–190 °C; R_f 0.63 (ethyl acetate); IR (KBr, cm^{-1}): 3343 (NH), 1708 (C=O), 1547 (C=N); ^{1}H NMR ($CDCl_3$): δ 2.39 (s, 3H, Ar–CH_3), 6.57 (d, J = 8.4 Hz, 1H, CO–CH), 7.38 (d, J = 6.8 Hz, 1H, CH–Ar), 7.52–8.18 (m, 7H, Ar–H), 13.14 (s, 1H, NH); EI-MS: m/z $[M+H]^+$ 330; Anal. Calcd for $C_{17}H_{13}ClN_2OS$: C, 62.10; H, 3.98; N, 8.52; S, 9.75. Found: C, 62.12; H, 3.97; N, 8.51; S, 9.76.

*6.2.1.21. 6-Methyl-[3-(4-hydroxyphenyl)-prop-2-eneamido]benzothiazole (**29**).* Pale white crystals; Yield: 56%; mp 221–223 °C; R_f 0.57 (ethyl acetate); IR (KBr, cm^{-1}): 3545 (OH), 3304 (NH), 1693 (C=O), 1564 (C=N); ^{1}H NMR ($CDCl_3$): δ 2.44 (s, 3H, Ar–CH_3), 6.73 (d, J = 8.1 Hz, 1H, CO–CH), 7.31 (d, J = 6.4 Hz, 1H, CH–Ar), 7.63–8.37 (m, 7H, Ar–H), 9.36 (s, 1H, OH), 12.52 (s, 1H, NH); EI-MS: m/z $[M+H]^+$ 312; Anal. Calcd for $C_{17}H_{14}N_2O_2S$: C, 65.79; H, 4.55; N, 9.03; S, 10.33. Found: C, 65.81; H, 4.54; N, 9.02; S, 10.34.

*6.2.1.22. 6-Methyl-[3-(3-hydroxy-4-methoxyphenyl)-prop-2-eneamido]benzothiazole (**30**).* Pale brown solid; Yield: 67%; mp 198–200 °C; R_f 0.64 (ethyl acetate); IR (KBr, cm^{-1}): 3580 (OH), 3352 (NH), 1718 (C=O), 1573 (C=N); ^{1}H NMR ($CDCl_3$): δ 2.36 (s, 3H, Ar–CH_3), 3.82 (s, 3H, Ar–OCH_3), 6.53 (d, J = 7.7 Hz, 1H, CO–CH), 7.17 (d, J = 6.4 Hz, 1H, CH–Ar), 7.62–8.27 (m, 6H, Ar–H), 9.67 (s, 1H, OH), 13.06 (s, 1H, NH); EI-MS: m/z $[M+H]^+$ 342; Anal. Calcd for $C_{18}H_{16}N_2O_3S$: C, 63.51; H, 4.74; N, 8.23; S, 9.42. Found: C, 63.53; H, 4.73; N, 8.24; S, 9.41.

*6.2.1.23. 6-Methyl-[3-(furan-2-yl)-prop-2-eneamido]benzothiazole (**31**).* Pale reddish-brown solid; Yield: 56%; mp 236–238 °C; R_f 0.67 (ethyl acetate); IR (KBr, cm^{-1}): 3324 (NH), 1704 (C=O), 1552 (C=N); ^{1}H NMR ($CDCl_3$): δ 2.43 (s, 3H, Ar–CH_3), 6.57 (d, J = 7.5 Hz, 1H, CO–CH), 7.26 (d, J = 6.7 Hz, 1H, CH–Ar), 7.78–8.32 (m, 6H,

Ar–H), 12.56 (s, 1H, NH); EI-MS: m/z $[M+H]^+$ 286; Anal. Calcd for $C_{15}H_{12}N_2O_2S$: C, 63.36; H, 4.25; N, 9.85; S, 11.28. Found: C, 63.37; H, 4.24; N, 9.85; S, 11.26.

*6.2.1.24. 6-Methyl-[3-(4-methoxyphenyl)-prop-2-eneamido]benzothiazole (**32**).* Pale yellow crystalline solid; Yield: 52%; mp 216–218 °C; R_f 0.61 (ethyl acetate); IR (KBr, cm^{-1}): 3298 (NH), 1715 (C=O), 1568 (C=N); ^1H NMR ($CDCl_3$): δ 2.53 (s, 3H, Ar–CH_3), 3.76 (s, 3H, Ar–OCH_3), 6.64 (d, $J = 8.2$ Hz, 1H, CO–CH), 7.26 (d, $J = 7.3$ Hz, 1H, CH–Ar), 7.58–8.13 (m, 7H, Ar–H), 12.86 (s, 1H, NH); EI-MS: m/z $[M+H]^+$ 326; Anal. Calcd for $C_{18}H_{16}N_2O_2S$: C, 66.64; H, 4.97; N, 8.64; S, 9.88. Found: C, 66.65; H, 4.96; N, 8.65; S, 9.86.

*6.2.2. General synthesis of 6-substituted-2-[(1-acetyl-5-substituted)-2-pyrazolin-3-yl]aminobenzothiazole (**33**–**56**)*

To a solution of appropriate 6-substituted-[3-substituted-prop-2-eneamido]-benzothiazoles **9**–**32** (0.01 mol) in dry ethanol (40 ml), hydrazine hydrate (99%, 0.02 mol) and few drops of glacial acetic acid were added. The reaction mixture was refluxed for 6–8 h. The excess solvent was distilled off in vacuum and the remaining mixture was poured onto ice–water. The residue was filtered, washed with water dried and recrystallized from ethanol (70%) to obtain 6-substituted-2-[(1-acetyl-5-substituted)-2-pyrazolin-3-yl]aminobenzothiazole **33**–**56**.

*6.2.2.1. 2-[(1-Acetyl-5-phenyl)-2-pyrazolin-3-yl]aminobenzothiazole (**33**).* White crystals; Yield: 73%; mp 182–184 °C; R_f 0.57 (ethyl acetate); IR (KBr, cm^{-1}): 3356 (NH), 1716 (C=O), 1552 (C=N), 1485 (N–N), 1120 (C–N); ^1H NMR ($CDCl_3$): δ 2.08 (s, 3H, CO–CH_3), 3.12 (dd, 1H, H_A, $J_{AB} = 16.84$ Hz, $J_{AX} = 6.42$ Hz), 3.38 (dd, 1H, H_B, $J_{AB} = 16.84$ Hz, $J_{BX} = 10.23$ Hz), 5.42 (dd, 1H, H_X, $J_{AX} = 7.86$ Hz, $J_{BX} = 11.4$ Hz), 7.56–7.86 (m, 9H, Ar–H), 8.80 (s, 1H, NH); EI-MS: m/z $[M+H]^+$ 317; Anal. Calcd for $C_{18}H_{16}N_4OS$: C, 64.26; H, 4.79; N, 16.65; S, 9.53. Found: C, 64.22; H, 4.81; N, 16.62; S, 9.55.

*6.2.2.2. 2-[(1-Acetyl-5-(4-chlorophenyl))-2-pyrazolin-3-yl]aminobenzothiazole (**34**).* White crystals; Yield: 59%; mp 196–198 °C; R_f 0.68 (ethyl acetate); IR (KBr, cm^{-1}): 3342 (NH), 1705 (C=O), 1562 (C=N), 1497 (N–N), 1110 (C–N); ^1H NMR ($CDCl_3$): δ 2.15 (s, 3H, CO–CH_3), 3.08 (dd, 1H, H_A, $J_{AB} = 16.26$ Hz, $J_{AX} = 6.12$ Hz), 3.95 (dd, 1H, H_B, $J_{AB} = 16.34$ Hz, $J_{BX} = 9.37$ Hz), 5.06 (dd, 1H, H_X, $J_{AX} = 6.4$ Hz, $J_{BX} = 10.59$ Hz), 7.76–8.10 (m, 8H, Ar–H), 8.56 (s, 1H, NH); EI-MS: m/z $[M+H]^+$ 372; Anal. Calcd for $C_{18}H_{15}ClN_4OS$: C, 58.30; H, 4.08; N, 15.11; S, 8.65. Found: C, 58.33; H, 4.11; N, 15.08; S, 8.63.

*6.2.2.3. 2-[(1-Acetyl-5-(4-hydroxyphenyl))-2-pyrazolin-3-yl]aminobenzothiazole (**35**).* White crystals; Yield: 63%; mp 219–221 °C; R_f 0.54 (ethyl acetate); IR (KBr, cm^{-1}): 3540 (OH), 3364 (NH), 1695 (C=O), 1570 (C=N), 1497 (N–N), 1088 (C–N); ^1H NMR ($CDCl_3$): δ 2.10 (s, 3H, CO–CH_3), 2.95 (dd, 1H, H_A, $J_{AB} = 16.67$ Hz, $J_{AX} = 7.9$ Hz), 3.36 (dd, 1H, H_B, $J_{AB} = 16.85$ Hz, $J_{BX} = 11.16$ Hz), 5.54 (dd, 1H, H_X, $J_{AX} = 7.24$ Hz, $J_{BX} = 11.07$ Hz), 7.46–7.92 (m, 8H, Ar–H), 8.76 (s, 1H, NH), 9.87 (s, 1H, OH); EI-MS: m/z $[M+H]^+$ 354; Anal. Calcd for $C_{18}H_{16}N_4O_2S$: C, 61.35; H, 4.58; N, 15.90; S, 9.10. Found: C, 61.32; H, 4.54; N, 15.93; S, 9.11.

*6.2.2.4. 2-[(1-Acetyl-5-(3-hydroxy-4-methoxyphenyl))-2-pyrazolin-3-yl]aminobenzothiazole (**36**).* Brown crystals; Yield: 72%; mp 197–199 °C; R_f 0.34 (ethyl acetate); IR (KBr, cm^{-1}): 3620 (OH), 3323 (NH), 1668 (C=O), 1552 (C=N), 1492 (N–N), 1105 (C–N); ^1H NMR ($CDCl_3$): δ 2.15 (s, 3H, CO–CH_3), 3.05 (dd, 1H, H_A, $J_{AB} = 17.22$ Hz, $J_{AX} = 6.53$ Hz), 3.48 (dd, 1H, H_B, $J_{AB} = 17.76$ Hz, $J_{BX} = 10.34$ Hz), 3.84 (s, 3H, Ar–OCH_3), 5.54 (dd, 1H, H_X, $J_{AX} = 6.98$ Hz, $J_{BX} = 11.12$ Hz), 7.82–8.23 (m, 8H, Ar–H), 8.85 (s, 1H, NH), 9.46 (s, 1H, OH); EI-MS: m/z $[M+H]^+$ 384; Anal. Calcd for $C_{19}H_{18}N_4O_3S$: C, 59.67; H, 4.74; N, 14.65; S, 8.38. Found: C, 59.61; H, 4.78; N, 14.62; S, 8.34.

*6.2.2.5. 2-[(1-Acetyl-5-(furan-2-yl))-2-pyrazolin-3-yl]aminobenzothiazole (**37**).* Pale brown crystals; Yield: 78%; mp 244–246 °C; R_f 0.57 (ethyl acetate); IR (KBr, cm^{-1}): 3290 (NH), 1710 (C=O), 1564 (C=N), 1480 (N–N), 1125 (C–N); ^1H NMR ($CDCl_3$): δ 2.21 (s, 3H, CO–CH_3), 2.98 (dd, 1H, H_A, $J_{AB} = 17.92$ Hz, $J_{AX} = 6.33$ Hz), 3.57 (dd, 1H, H_B, $J_{AB} = 16.68$ Hz, $J_{BX} = 10.24$ Hz), 5.72 (dd, 1H, H_X, $J_{AX} = 6.75$ Hz, $J_{BX} = 9.68$ Hz), 7.64–8.09 (m, 7H, Ar–H), 9.10 (s, 1H, NH); EI-MS: m/z $[M+H]^+$ 328; Anal. Calcd for $C_{16}H_{14}N_4O_2S$: C, 58.88; H, 4.32; N, 17.17; S, 9.82. Found: C, 58.81; H, 4.28; N, 17.25; S, 9.84.

*6.2.2.6. 2-[(1-Acetyl-5-(4-methoxyphenyl))-2-pyrazolin-3-yl]aminobenzothiazole (**38**).* White crystals; Yield: 57%; mp 211–213 °C; R_f 0.38 (ethyl acetate); IR (KBr, cm^{-1}): 3340 (NH), 1690 (C=O), 1570 (C=N), 1510 (N–N), 1095 (C–N); ^1H NMR ($CDCl_3$): δ 2.14 (s, 3H, CO–CH_3), 3.14 (dd, 1H, H_A, $J_{AB} = 16.85$ Hz, $J_{AX} = 6.43$ Hz), 3.74 (s, 3H, OCH_3), 3.92 (dd, 1H, H_B, $J_{AB} = 17.46$ Hz, $J_{BX} = 9.51$ Hz), 5.85 (dd, 1H, H_X, $J_{AX} = 7.12$ Hz, $J_{BX} = 11.56$ Hz), 7.76–7.96 (m, 8H, Ar–H), 8.72 (s, 1H, NH); EI-MS: m/z $[M+H]^+$ 368; Anal. Calcd for $C_{19}H_{18}N_4O_2S$: C, 62.28; H, 4.95; N, 15.29; S, 8.75. Found: C, 62.22; H, 4.99; N, 15.34; S, 8.74.

*6.2.2.7. 6-Chloro-2-[(1-acetyl-5-phenyl)-2-pyrazolin-3-yl]aminobenzothiazole (**39**).* Pale yellow solid; Yield: 63%; mp 242–244 °C; R_f 0.52 (ethyl acetate); IR (KBr, cm^{-1}): 3315 (NH), 1710 (C=O), 1545 (C=N), 1490 (N–N), 1110 (C–N); ^1H NMR ($CDCl_3$): δ 2.11 (s, 3H, CO–CH_3), 3.14 (dd, 1H, H_A, $J_{AB} = 17.02$ Hz, $J_{AX} = 6.32$ Hz), 3.79 (dd, 1H, H_B, $J_{AB} = 16.96$ Hz, $J_{BX} = 10.53$ Hz), 5.08 (dd, 1H, H_X, $J_{AX} = 6.44$ Hz, $J_{BX} = 11.31$ Hz), 7.45–7.88 (m, 8H, Ar–H), 8.65 (s, 1H, NH); EI-MS: m/z $[M+H]^+$ 371; Anal. Calcd for $C_{18}H_{15}ClN_4OS$: C, 58.30; H, 4.08; N, 15.11; S, 8.65. Found: C, 58.22; H, 4.14; N, 15.04; S, 8.69.

*6.2.2.8. 6-Chloro-2-[(1-acetyl-5-(4-chlorophenyl))-2-pyrazolin-3-yl]-aminobenzothiazole (**40**).* White crystals; Yield: 73%; mp 287–289 °C; R_f 0.43 (ethyl acetate); IR (KBr, cm^{-1}): 3367 (NH), 1685 (C=O), 1560 (C=N), 1510 (N–N), 1090 (C–N); ^1H NMR ($CDCl_3$): δ 2.20 (s, 3H, CO–CH_3), 2.96 (dd, 1H, H_A, $J_{AB} = 16.24$ Hz, $J_{AX} = 7.4$ Hz), 3.82 (dd, 1H, H_B, $J_{AB} = 16.45$ Hz, $J_{BX} = 9.63$ Hz), 5.17 (dd, 1H, H_X, $J_{AX} = 7.43$ Hz, $J_{BX} = 10.23$ Hz), 7.78–8.30 (m, 7H, Ar–H), 8.87 (s, 1H, NH); EI-MS: m/z $[M+H]^+$ 407; Anal. Calcd for $C_{18}H_{14}Cl_2N_4OS$: C, 53.34; H, 3.48; N, 13.82; S, 7.91. Found: C, 53.26; H, 3.43; N, 13.88; S, 7.94.

*6.2.2.9. 6-Chloro-2-[(1-acetyl-5-(4-hydroxyphenyl))-2-pyrazolin-3-yl]aminobenzothiazole (**41**).* Pale brown crystals; Yield: 57%; mp 224–226 °C; R_f 0.53 (ethyl acetate); IR (KBr, cm^{-1}): 3540 (OH), 3290 (NH), 1710 (C=O), 1560 (C=N), 1490 (N–N), 1110 (C–N); ^1H NMR ($CDCl_3$): δ 2.22 (s, 3H, CO–CH_3), 3.09 (dd, 1H, H_A, $J_{AB} = 17.86$ Hz, $J_{AX} = 6.32$ Hz), 3.54 (dd, 1H, H_B, $J_{AB} = 17.21$ Hz, $J_{BX} = 9.65$ Hz), 5.28 (dd, 1H, H_X, $J_{AX} = 6.88$ Hz, $J_{BX} = 10.18$ Hz), 7.40–7.82 (m, 7H, Ar–H), 8.51 (s, 1H, NH), 10.11 (s, 1H, OH); EI-MS: m/z $[M+H]^+$ 388; Anal. Calcd for $C_{18}H_{15}ClN_4O_2S$: C, 55.88; H, 3.91; N, 14.48; S, 8.29. Found: C, 55.76; H, 3.88; N, 14.52; S, 8.34.

*6.2.2.10. 6-Chloro-2-[(1-acetyl-5-(3-hydroxy4-methoxyphenyl))-2-pyrazolin-3-yl]-aminobenzothiazole (**42**).* Pale brown crystals; Yield: 65%; mp 212–214 °C; R_f 0.71 (ethyl acetate); IR (KBr, cm^{-1}): 3630 (OH), 3385 (NH), 1680 (C=O), 1575 (C=N), 1495 (N–N), 1120 (C–N); ^1H NMR ($CDCl_3$): δ 2.15 (s, 3H, CO–CH_3), 3.12 (dd, 1H, H_A, $J_{AB} = 16.65$ Hz, $J_{AX} = 7.4$ Hz), 3.37 (dd, 1H, H_B, $J_{AB} = 16.82$ Hz, $J_{BX} = 11.17$ Hz), 3.80 (s, 3H, OCH_3), 5.53 (dd, 1H, H_X, $J_{AX} = 7.24$ Hz, $J_{BX} = 11.16$ Hz), 7.63–8.12 (m, 6H, Ar–H), 8.76 (s, 1H, NH), 10.18 (s, 1H, OH); EI-MS: m/z $[M+H]^+$ 418; Anal. Calcd for $C_{19}H_{17}ClN_4O_3S$: C, 54.74; H, 4.11; N, 13.44; S, 7.69. Found: C, 54.67; H, 4.07; N, 13.42; S, 7.75.

*6.2.2.11. 6-Chloro-2-[(1-acetyl-5-(furan-2-yl))-2-pyrazolin-3-yl]aminobenzothiazole (**43**).* Pale brown solid; Yield: 61%; mp 227–229 °C; R_f 0.56 (ethyl acetate); IR (KBr, cm^{-1}): 3340 (NH), 1670 (C=O), 1550 (C=N), 1482 (N–N), 1090 (C–N); ^1H NMR ($CDCl_3$): δ 2.07 (s, 3H, CO–CH_3), 3.11 (dd, 1H, H_A, $J_{AB} = 16.05$ Hz, $J_{AX} = 7.28$ Hz), 3.82 (dd, 1H, H_B, $J_{AB} = 16.17$ Hz, $J_{BX} = 11.19$ Hz), 5.24 (dd, 1H, H_X, $J_{AX} = 7.54$ Hz, $J_{BX} = 11.24$ Hz), 7.46–7.98 (m, 6H, Ar–H), 9.11 (s, 1H, NH); EI-MS: m/z $[M+H]^+$ 362; Anal. Calcd for $C_{16}H_{13}ClN_4O_2S$: C, 53.26; H, 3.63; N, 15.53; S, 8.89. Found: C, 53.18; H, 3.54; N, 15.60; S, 8.93.

*6.2.2.12. 6-Chloro-2-[(1-acetyl-5-(4-methoxyphenyl))-2-pyrazolin-3-yl]aminobenzothiazole (**44**).* Pale white crystals; Yield: 72%; mp 192–194 °C; R_f 0.66 (ethyl acetate); IR (KBr, cm^{-1}): 3323 (NH), 1710 (C=O), 1565 (C=N), 1510 (N–N), 1085 (C–N); ^1H NMR ($CDCl_3$): δ 2.24 (s, 3H, CO–CH_3), 3.12 (dd, 1H, H_A, $J_{AB} = 17.42$ Hz, $J_{AX} = 6.44$ Hz), 3.71 (dd, 1H, H_B, $J_{AB} = 17.56$ Hz, $J_{BX} = 11.5$ Hz), 3.88 (s, 3H, OCH_3), 5.11 (dd, 1H, H_X, $J_{AX} = 7.92$ Hz, $J_{BX} = 9.45$ Hz), 7.67–8.21 (m, 7H, Ar–H), 9.05 (s, 1H, NH); EI-MS: m/z $[M+H]^+$ 402; Anal. Calcd for $C_{19}H_{17}ClN_4O_2S$: C, 56.93; H, 4.27; N, 13.98; S, 8.00. Found: C, 56.81; H, 4.31; N, 13.92; S, 7.98.

*6.2.2.13. 6-Nitro-2-[(1-acetyl-5-phenyl)-2-pyrazolin-3-yl]aminobenzothiazole (**45**).* Yellow solid; Yield: 63%; mp 210–212 °C; R_f 0.45 (ethyl acetate); IR (KBr, cm^{-1}): 3293 (NH), 1670 (C=O), 1560 (C=N), 1490 (N–N), 1110 (C–N); ^1H NMR ($CDCl_3$): δ 2.08 (s, 3H, CO–CH_3), 3.06 (dd, 1H, H_A, $J_{AB} = 17.54$ Hz, $J_{AX} = 6.23$ Hz), 3.42 (dd, 1H, H_B, $J_{AB} = 17.94$ Hz, $J_{BX} = 10.02$ Hz), 5.84 (dd, 1H, H_X, $J_{AX} = 7.32$ Hz, $J_{BX} = 11.09$ Hz), 7.68–8.12 (m, 8H, Ar–H), 8.77 (s, 1H, NH); EI-MS: m/z $[M+H]^+$ 383; Anal. Calcd for $C_{18}H_{15}N_5O_3S$: C, 56.68; H, 3.96; N, 18.36; S, 8.41. Found: C, 56.54; H, 3.91; N, 18.44; S, 8.45.

*6.2.2.14. 6-Nitro-2-[(1-acetyl-5-(4-chlorophenyl))-2-pyrazolin-3-yl]aminobenzothiazole (**46**).* Yellow solid; Yield: 56%; mp 238–240 °C; R_f 0.63 (ethyl acetate); IR (KBr, cm^{-1}): 3377 (NH), 1715 (C=O), 1580 (C=N), 1495 (N–N), 1095 (C–N); ^1H NMR ($CDCl_3$): δ 2.21 (s, 3H, CO–CH_3), 3.08 (dd, 1H, H_A, $J_{AB} = 17.22$ Hz, $J_{AX} = 7.65$ Hz), 3.81 (dd, 1H, H_B, $J_{AB} = 16.24$ Hz, $J_{BX} = 9.82$ Hz), 5.08 (dd, 1H, H_X, $J_{AX} = 7.15$ Hz, $J_{BX} = 10.85$ Hz), 7.46–8.02 (m, 7H, Ar–H), 9.15 (s, 1H, NH); EI-MS: m/z $[M+H]^+$ 417; Anal. Calcd for $C_{18}H_{14}ClN_5O_3S$: C, 51.99; H, 3.39; N, 16.84; S, 7.71. Found: C, 51.87; H, 3.45; N, 16.79; S, 7.73.

*6.2.2.15. 6-Nitro-2-[(1-acetyl-5-(4-hydroxyphenyl))-2-pyrazolin-3-yl]-aminobenzothiazole (**47**).* Yellow solid; Yield: 62%; mp 285–287 °C; R_f 0.43 (ethyl acetate); IR (KBr, cm^{-1}): 3615 (OH), 3290 (NH), 1690 (C=O), 1565 (C=N), 1480 (N–N), 1115 (C–N); ^1H NMR ($CDCl_3$): δ 2.14 (s, 3H, CO–CH_3), 3.15 (dd, 1H, H_A, $J_{AB} = 17.98$ Hz, $J_{AX} = 6.38$ Hz), 3.44 (dd, 1H, H_B, $J_{AB} = 17.46$ Hz, $J_{BX} = 9.64$ Hz), 5.31 (dd, 1H, H_X, $J_{AX} = 7.12$ Hz, $J_{BX} = 11.41$ Hz), 7.58–7.96 (m, 7H, Ar–H), 8.66 (s, 1H, NH), 9.53 (s, 1H, OH); EI-MS: m/z $[M+H]^+$ 399; Anal. Calcd for $C_{18}H_{15}N_5O_4S$: C, 54.40; H, 3.80; N, 17.62; S, 8.07. Found: C, 54.32; H, 3.74; N, 17.68; S, 8.11.

*6.2.2.16. 6-Nitro-2-[(1-acetyl-5-(3-hydroxy-4-methoxyphenyl))-2-pyrazolin-3-yl]-aminobenzothiazole (**48**).* Yellow solid; Yield: 72%; mp 274–276 °C; R_f 0.56 (ethyl acetate); IR (KBr, cm^{-1}): 3585 (OH), 3344 (NH), 1724 (C=O), 1578 (C=N), 1482 (N–N), 1090 (C–N); ^1H NMR ($CDCl_3$): δ 2.23 (s, 3H, CO–CH_3), 3.11 (dd, 1H, H_A, $J_{AB} = 17.98$ Hz, $J_{AX} = 6.24$ Hz), 3.52 (dd, 1H, H_B, $J_{AB} = 17.07$ Hz, $J_{BX} = 9.54$ Hz), 3.72 (s, 3H, OCH_3), 5.13 (dd, 1H, H_X, $J_{AX} = 6.76$ Hz, $J_{BX} = 9.09$ Hz), 7.65–8.20 (m, 6H, Ar–H), 9.11 (s, 1H, NH), 10.18 (s, 1H, OH); EI-MS: m/z $[M+H]^+$ 429; Anal. Calcd for $C_{19}H_{17}N_5O_5S$: C, 53.39; H, 4.01; N, 16.38; S, 7.50. Found: C, 53.29; H, 4.06; N, 16.34; S, 7.54.

*6.2.2.17. 6-Nitro-2-[(1-acetyl-5-(furan-2-yl))-2-pyrazolin-3-yl]aminobenzothiazole (**49**).* Yellow solid; Yield: 57%; mp 281–283 °C; R_f 0.43 (ethyl acetate); IR (KBr, cm^{-1}): 3368 (NH), 1710 (C=O), 1562 (C=N), 1496 (N–N), 1112 (C–N); ^1H NMR ($CDCl_3$): δ 2.16 (s, 3H, CO–CH_3), 3.14 (dd, 1H, H_A, $J_{AB} = 17.64$ Hz, $J_{AX} = 6.53$ Hz), 3.82 (dd, 1H, H_B, $J_{AB} = 17.32$ Hz, $J_{BX} = 10.16$ Hz), 5.12 (dd, 1H, H_X, $J_{AX} = 6.87$ Hz, $J_{BX} = 10.18$ Hz), 7.48–7.92 (m, 6H, Ar–H), 8.55 (s, 1H, NH); EI-MS: m/z $[M+H]^+$ 373; Anal. Calcd for $C_{16}H_{13}N_5O_4S$: C, 51.75; H, 3.53; N, 18.86; S, 8.63. Found: C, 51.64; H, 3.56; N, 18.92; S, 8.60.

*6.2.2.18. 6-Nitro-2-[(1-acetyl-5-(4-methoxyphenyl))-2-pyrazolin-3-yl]-aminobenzothiazole (**50**).* Yellow solid; Yield: 76%; mp 244–246 °C; R_f 0.61 (ethyl acetate); IR (KBr, cm^{-1}): 3355 (NH), 1690 (C=O), 1546 (C=N), 1510 (N–N), 1105 (C–N); ^1H NMR ($CDCl_3$): δ 2.08 (s, 3H, CO–CH_3), 2.97 (dd, 1H, H_A, $J_{AB} = 16.62$ Hz, $J_{AX} = 7.8$ Hz), 3.32 (dd, 1H, H_B, $J_{AB} = 16.85$ Hz, $J_{BX} = 11.17$ Hz), 3.70 (s, 1H, OCH_3), 5.51 (dd, 1H, H_X, $J_{AX} = 7.27$ Hz, $J_{BX} = 11.09$ Hz), 7.52–7.97 (m, 7H, Ar–H), 9.10 (s, 1H, NH); EI-MS: m/z $[M+H]^+$ 413; Anal. Calcd for $C_{19}H_{17}N_5O_4S$: C, 55.47; H, 4.16; N, 17.02; S, 7.79. Found: C, 55.41; H, 4.13; N, 17.05; S, 7.81.

*6.2.2.19. 6-Methyl-2-[(1-acetyl-5-phenyl)-2-pyrazolin-3-yl]aminobenzothiazole (**51**).* White crystals; Yield: 61%; mp 204–206 °C; R_f 0.68 (ethyl acetate); IR (KBr, cm^{-1}): 3371 (NH), 1723 (C=O), 1557 (C=N), 1490 (N–N), 1092 (C–N); ^1H NMR ($CDCl_3$): δ 2.24 (s, 3H, CO–CH_3), 2.45 (s, 3H, Ar–CH_3), 3.14 (dd, 1H, H_A, $J_{AB} = 17.23$ Hz, $J_{AX} = 7.52$ Hz), 3.87 (dd, 1H, H_B, $J_{AB} = 17.92$ Hz, $J_{BX} = 10.22$ Hz), 5.43 (dd, 1H, H_X, $J_{AX} = 6.53$ Hz, $J_{BX} = 10.54$ Hz), 7.74–8.27 (m, 8H, Ar–H), 8.72 (s, 1H, NH); EI-MS: m/z $[M+H]^+$ 352; Anal. Calcd for $C_{19}H_{18}N_4OS$: C, 65.12; H, 5.18; N, 15.99; S, 9.15. Found: C, 65.03; H, 5.12; N, 16.05; S, 9.20.

*6.2.2.20. 6-Methyl-2-[(1-acetyl-5-(4-chlorophenyl))-2-pyrazolin-3-yl]-aminobenzothiazole (**52**).* Pale white crystals; Yield: 73%; mp 187–189 °C; R_f 0.51 (ethyl acetate); IR (KBr, cm^{-1}): 3292 (NH), 1705 (C=O), 1564 (C=N), 1485 (N–N), 1115 (C–N); ^1H NMR ($CDCl_3$): δ 2.17 (s, 3H, CO–CH_3), 2.38 (s, 3H, Ar–CH_3), 3.12 (dd, 1H, H_A, $J_{AB} = 17.84$ Hz, $J_{AX} = 6.54$ Hz), 3.64 (dd, 1H, H_B, $J_{AB} = 16.98$ Hz, $J_{BX} = 10.76$ Hz), 5.12 (dd, 1H, H_X, $J_{AX} = 7.23$ Hz, $J_{BX} = 9.87$ Hz), 7.56–8.12 (m, 7H, Ar–H), 9.14 (s, 1H, NH); EI-MS: m/z $[M+H]^+$ 386; Anal. Calcd for $C_{19}H_{17}ClN_4OS$: C, 59.29; H, 4.45; N, 14.56; S, 8.33. Found: C, 59.23; H, 4.47; N, 14.59; S, 8.37.

*6.2.2.21. 6-Methyl-2-[(1-acetyl-5-(4-hydroxyphenyl))-2-pyrazolin-3-yl]aminobenzothiazole (**53**).* Pale yellow solid; Yield: 65%; mp 232–234 °C; R_f 0.46 (ethyl acetate); IR (KBr, cm^{-1}): 3564 (OH), 3368 (NH), 1723 (C=O), 1548 (C=N), 1497 (N–N), 1084 (C–N); ^1H NMR ($CDCl_3$): δ 2.25 (s, 3H, CO–CH_3), 2.46 (s, 3H, Ar–CH_3), 3.09 (dd, 1H, H_A, $J_{AB} = 17.34$ Hz, $J_{AX} = 6.86$ Hz), 3.82 (dd, 1H, H_B, $J_{AB} = 17.58$ Hz, $J_{BX} = 9.86$ Hz), 5.64 (dd, 1H, H_X, $J_{AX} = 6.24$ Hz, $J_{BX} = 9.21$ Hz), 7.66–8.30 (m, 7H, Ar–H), 8.86 (s, 1H, NH), 9.57 (s, 1H, OH); EI-MS: m/z $[M+H]^+$ 368; Anal. Calcd for $C_{19}H_{18}N_4O_2S$: C, 62.28; H, 4.95; N, 15.29; S, 8.75. Found: C, 62.17; H, 4.91; N, 15.34; S, 8.78.

*6.2.2.22. 6-Methyl-2-[(1-acetyl-5-(3-hydroxy-4-methoxyphenyl))-2-pyrazolin-3-yl]-aminobenzothiazole (**54**).* Pale white crystals; Yield: 72%; mp 251–253 °C; R_f 0.52 (ethyl acetate); IR (KBr, cm^{-1}): 3624 (OH), 3292 (NH), 1684 (C=O), 1576 (C=N), 1482 (N–N), 1124 (C–N); ^1H NMR ($CDCl_3$): δ 2.12 (s, 3H, CO–CH_3), 2.54 (s, 3H, Ar–CH_3), 2.96 (dd, 1H, H_A, $J_{AB} = 17.85$ Hz, $J_{AX} = 6.75$ Hz), 3.42 (dd, 1H, H_B, $J_{AB} = 16.52$ Hz, $J_{BX} = 9.19$ Hz), 3.84 (s, 3H, Ar–OCH_3), 5.74 (dd, 1H, H_X, $J_{AX} = 7.81$ Hz, $J_{BX} = 9.16$ Hz), 7.40–7.85 (m, 6H, Ar–H), 9.11 (s, 1H, NH), 9.86 (s, 1H, OH); EI-MS: m/z $[M+H]^+$ 398; Anal. Calcd for

$C_{20}H_{20}N_4O_3S$: C, 60.59; H, 5.08; N, 14.13; S, 8.09. Found: C, 60.51; H, 5.05; N, 14.16; S, 8.12.

*6.2.2.23. 6-Methyl-2-[(1-acetyl-5-(furan-2-yl))-2-pyrazolin-3-yl]aminobenzothiazole (**55**).* Pale yellow crystals; Yield: 56%; mp 208–210 °C; R_f 0.63 (ethyl acetate); IR (KBr, cm^{-1}): 3355 (NH), 1710 (C═O), 1545 (C═N), 1470 (N–N), 1090 (C–N); ^{1}H NMR ($CDCl_3$): δ 2.18 (s, 3H, CO–CH_3), 2.47 (s, 3H, Ar–CH_3), 3.09 (dd, 1H, H_A, $J_{AB} = 17.32$ Hz, $J_{AX} = 6.24$ Hz), 3.52 (dd, 1H, H_B, $J_{AB} = 17.87$ Hz, $J_{BX} = 9.53$ Hz), 5.76 (dd, 1H, H_X, $J_{AX} = 7.63$ Hz, $J_{BX} = 10.84$ Hz), 7.52–7.96 (m, 6H, Ar–H), 8.76 (s, 1H, NH); EI-MS: m/z $[M + H]^+$ 342; Anal. Calcd for $C_{17}H_{16}N_4O_2S$: C, 59.98; H, 4.74; N, 16.46; S, 9.42. Found: C, 59.91; H, 4.72; N, 16.53; S, 9.46.

6.2.2.24. 6-Methyl-2-[(1-acetyl-5-(4-methoxyphenyl))-2-pyrazolin-3-yl]aminobenzothiazole. (**56**)White crystals; Yield: 71%; mp 235–237 °C; R_f 0.54 (ethyl acetate); IR (KBr, cm^{-1}): 3365 (NH), 1686 (C═O), 1552 (C═N), 1486 (N–N), 1110 (C–N); ^{1}H NMR ($CDCl_3$): δ 2.14 (s, 3H, CO–CH_3), 2.54 (s, 3H, Ar–CH_3), 3.08 (dd, 1H, H_A, $J_{AB} = 17.12$ Hz, $J_{AX} = 6.86$ Hz), 3.56 (dd, 1H, H_B, $J_{AB} = 16.54$ Hz, $J_{BX} = 10.26$ Hz), 3.77 (s, 3H, Ar–OCH_3), 5.84 (dd, 1H, H_X, $J_{AX} = 7.35$ Hz, $J_{BX} = 11.41$ Hz), 7.63–8.16 (m, 7H, Ar–H), 8.87 (s, 1H, NH); EI-MS: m/z $[M + H]^+$ 382; Anal. Calcd for $C_{20}H_{20}N_4O_2S$: C, 63.14; H, 5.30; N, 14.73; S, 8.43 Found: C, 63.08; H, 5.32; N, 14.69; S, 8.48.

6.3. Anticonvulsant activity

The anticonvulsant activity was carried out on albino mice (20–25 g) of either sex or male albino rats (100–150 g) as experimental animals. The animals were housed under standard conditions and allowed free access to standard pellet diet and water (*ab libitum*). The test compounds and standard drug were suspended in 0.5% methyl cellulose/water mixture.

6.3.1. Maximum electroshock (MES) test

The test compounds were administered intraperitoneally (ip) at a dose of 20–1000 μmol/kg body weight. Maximum electroshock seizure were elicited using electroconvulsometer with a 60 cycle altering current of 50 mA for 0.25 s via ear clip electrode as per the reported procedure and effect was assessed at 0.5 h after administration by recording the tonic extension of the hind limbs at different doses. The reduction in time or absence of hind limb tonic extension of seizure is defined as protection. Median effective dose (ED_{50}) was calculated at the doses of test drugs until atleast three points were established in the range of 10–90% seizure protection or minimal observed neurotoxicity (Table 1).

6.3.2. Subcutaneous pentylenetetrazole (scPTZ) seizure threshold test

Pentylenetetrazole dissolved in 0.9% sodium chloride solution was administered in the posterior midline of the mice and the onset and severity of convulsion was noted for the control group. The test group was administered with the selected compounds 0.5 h prior to the administration of PTZ and the anticonvulsant activity was detected in terms of ED_{50} and is presented in Table 1.

6.3.3. Neurotoxicity screening

The neurotoxicity of all the test compounds was evaluated using rotorod test. Mice were trained to balance on the rotating rod (3.2 cm diameter) that rotates at 6 rpm. Trained animals were treated with test compounds at a dose of 20–1000 μmol/kg administered intraperitoneally. Neurotoxicity was determined by the inability of the animal to remain on the rod for 1 min. The results are represented as TD_{50} which are further used in the calculation of PI (TD_{50}/ED_{50}) (Table 1).

6.3.4. Behavioral activity

The activity was measured as digital score using actophotometer [34] with the ip administration of drug (100 μmol/kg) to mice. The mice were placed in the box and the behavior was noted for 10 min. Further, the animals were treated with the drug and after 0.5 h of drug administration the animal were re-tested. The activity score was noted and based on these results, % change was calculated and represented in Table 2.

6.3.5. Porsolt's swimpool test

The CNS depressant study was carried out using Porsolt's swimpool test [35]. The rats were placed in chamber containing water and subjected to a 15 min swimming session 24 h before the test. The rats were administered intraperitoneally at dose of 100 μmol/kg and 0.5 h before the test. The duration of immobility was recorded during the 5 min test period (Table 3).

6.3.6. Liver function test

The rats were divided into groups of six, and the control group received a basal diet and vehicle. The other groups were administered the test drug in a dose of 100 μmol/kg/day (in methyl cellulose) for 15 days. After the stipulated period, each animal was anesthetized and the blood was collected from the liver to assess the serum level of SGOT and SGPT (Table 4) according to the reported procedure [27].

6.4. 3D-QSAR analysis

6.4.1. Data set and biological activity

A set of 48 molecules (Table 1) was used for the generation of 3D-QSAR model. The data set was divided into a training set (29 molecules) and test set (19 molecules) based on the Tanimoto similarity coefficient [40]. All the biological activity data were converted to negative logarithmic molar concentration of ED_{50} values [$pED_{50} = -\log(ED_{50} \times 10^{-6})$] and used for 3D-QSAR studies.

6.4.2. Molecular modeling and PHASE methodology

The 3D-QSAR studies were carried out using PHASE version 3.0.110 implemented in the Maestro 8.5.111 modeling package (Schrödinger, Inc., LLC, New York, USA) installed on a Pentium IV 3.06 GHz PC with Linux OS (RedHat Enterprise WS 4.0). The structures of the molecules were built using structure drawing tool which was cleaned and minimized using LigPrep program to attach hydrogens and generate stereoisomers at neutral pH 7 using 'ionizer' subprogram. Conformer generation was carried out with Macromodel ligand torsion search using MMFs force field with implicit GB/SA distance dependent dielectric solvent model at cutoff root mean square deviation (RMSD) of 1 Å. The active and inactive threshold of 3.8 and 3.3, respectively, were applied to the training set. The pharmacophore feature sites for the molecules were assigned using a terminal box size of 1 Å and applying a set of features defined in PHASE as hydrogen-bond acceptor (A), hydrogen-bond donor (D), hydrophobic (H), negative ionic (N), positive ionic (P) and aromatic (R) with the requirement that all seven active matches. The common pharmacophore was generated by considering five sites that matches seven active ligands. Hypotheses were generated by a systematic variation of number of sites (n_{sites}) and the number of matching active compounds (n_{act}). With $n_{act} = n_{act-tot}$ initially ($n_{act-tot}$ is the total number of active compounds in the training set), n_{sites} was varied from 7 to 3 until atleast one hypotheses was found and scored successfully. If this failed, then n_{act} was decreased by one and the n_{sites} cycle was

repeated. The hypotheses were scored using default parameters for site, vector, volume, selectivity, number of matches and energy terms. The hypotheses that emerged from this process subsequently scored with respect to the three inactives, again with default parameters. Atom based 3D-QSAR models were generated for the hypotheses using the 29 member training set with four (4) PLS factor and a grid spacing of 1 Å.

6.4.3. PHASE QSAR statistics and model validation

The PHASE descriptors served as independent variables and activity values as dependent variables in deducing 3D-QSAR models by PLS regression analysis method. PHASE QSAR models do not use internal cross-validation techniques but rather uses distinct training and test sets. The true external test sets assist in the validation of 3D-QSAR model and helps in the generation of validation parameters like q^2 and r_p values. The predictive ability of each analysis was determined from a test of 19 ligands that were not included in the training set. The test set molecules were aligned and their activities were predicted by each PLS analysis. The statistical results are summarized in Table 5.

6.4.4. 3D-QSAR plots

The 3D-QSAR results can be visualized using 3D plots of crucial pharmacophore regions (Fig. 3 a–e). The cubes (region) that represent the model are displayed in the workspace and colored according to the sign of their coefficient values. The blue cubes refer to ligand region as positive coefficients in which the specific feature is important for the increase in activity, whereas the red cubes refers to negative coefficients indicating the same ligand feature substitution with decrease in activity.

Acknowledgements

We are grateful to Dr. P. Trivedi and C. Kartikeyan, Computational Chemistry Research Laboratory, RGPV, Bhopal for their help in carrying out the computational work. Also, we are thankful to Dr. Bhoomendra Bhongade, International Medical University, Kuala Lumpur, Malaysia for his help and valuable suggestions in manuscript revision.

References

[1] A.N. Prasad, C. Prasad, Genetic influences on the risk of epilepsy. in: J.M. Pellock, B.F. Bourgeols, W.E. Dodson (Eds.), Pediatric Epilepsy: Diagnosis and Therapy, third ed. Demos Publishers, New York, 2001, p. 117.
[2] J.O. McNamara, Drugs effective in the therapy of the epilepsies. in: J.G. Hardman, L.E. Limbird (Eds.), Goodman and Gilman's The Pharmacological Basis of Therapeutics. Mc Graw-Hill, New York, 2001, pp. 521–547.
[3] M.D. Daras, P.F. Bladin, M.J. Eadie, D. Millet, Epilepsy: historical perspectives. in: J. Engel, T. Pedley Jr. (Eds.), second ed., Epilepsy: A Comprehensive Textbook, vol. 1 Lippincott Williams and Wilkins, Philadelphia, 2007, p. 13.
[4] Secretariats of WHO/IBE/ILAE, Global Campaign Against Epilepsy, Atlas: Epilepsy Care in the World, Programme for Neurological Diseases and Neuroscience. Department of Mental Health and Substance Abuse, World Health Organization, Geneva, 2009.http://www.who.int/entity/mediacentre/factsheets/fs999/en.
[5] Annual report of the WHO/IBE/ILAE, Global Campaign Agianst Epilepsy Out of the Shadows. Paswerk Grafish, Hoofddorp, The Netherlands, 2003.http://www.who.int/entity/mental_health/management/globalepilepsycampaign/en.
[6] P. Yogeeswari, D. Sriram, R. Thirumurugan, J. Raghvendran, K. Sudan, R. Pavana, J. Stables, J. Med. Chem. 48 (2005) 6202–6211.
[7] K.J. Meader, J. Clin. Psychiatry 64 (2003) 30–34.
[8] H. Stefan, T. Feuerstein, Pharmacol. Ther. 113 (2007) 165–183.
[9] J.R. Pollard, J. French, Lancet Neurol. 5 (2006) 1064–1067.
[10] E.J. Donner, O.C. Snead III, NeuroRX 3 (2006) 170–180.
[11] M. Bialer, S.I. Johannessen, H.J. Kupferberg, R.H. Levy, E. Perucca, T. Tomson, Epilepsy Res. 61 (2004) 1–48.
[12] J.F. Wolfe, T.D. Greenwood, J.M. Mulheron, Expert Opin. Ther. Pat. 8 (1998) 361–381.
[13] G.A. Burdock, Encyclopedia of Food and Color Additives, Technology and Engineering, CRC Press, Boca Raton, FL, 1996, pp. 255.
[14] A.R. Carroll, P.J. Scheuer, J. Org. Chem. 55 (1990) 4426–4431.
[15] G.P. Gunawardana, S. Kohmoto, N.S. Burres, Tetrahedron Lett. 30 (1989) 4359–4362.
[16] G. Zitouni, S. Demirayak, A. Ozdemir, Z. Kaplancikli, M. Yildiz, Eur. J. Med. Chem. 39 (2003) 267–272.
[17] K.P. Bhusari, N.D. Amnerkar, P.B. Khedekar, M.K. Kale, R.P. Bhole, Asian J. Res. Chem. 1 (2008) 53–58.
[18] R.S. Chopade, R.H. Bahekar, P.B. Khedekar, K.P. Bhusari, A.R.R. Rao, Arch. Pharm. Pharm. Med. Chem. 8 (2002) 381–388.
[19] P. Yogeeswari, D. Srisam, L. Suniljit, S. Kumar, J. Stables, Eur. J. Med. Chem. 37 (2002) 231–236.
[20] P. Yogeeswari, D. Sriram, S. Mehta, D. Nigam, M. Kumar, S. Murugesan, J. Stables II, Farmaco 60 (2005) 1–5.
[21] N. Siddiqui, S. Pandeya, S. Khan, J. Stables, A. Rana, M. Alam, M. Arshad, M. Bhat, Bioorg. Med. Chem. Lett. 17 (2007) 255–259.
[22] N. Siddiqui, A. Rana, S. Khan, M. Bhat, S. Haque, Bioorg. Med. Chem. Lett. 17 (2007) 4178–4182.
[23] P. Jimonet, F. Audiau, M. Barreau, J. Blanchard, A. Boireau, Y. Bour, M. Colno, A. Doble, G. Doerflinger, C. Huu, M. Donat, J. Duchesne, P. Ganil, C. Gurmy, E. Honor, B. Just, R. Kerphirique, S. Gontier, P. Hubert, P. Laduron, J. Blevec, M. Meunier, J. Miquet, C. Nemecek, M. Pasquet, O. Piot, J. Pratt, J. Rataud, J. Reibaud, J. Stutzmann, S. Migani, J. Med. Chem. 42 (1999) 2828–2843.
[24] V. Michon, C. Penhoat, F. Tombret, J. Gillardin, F. Lepage, L. Berthon, Eur. J. Med. Chem. 30 (1995) 147–155.
[25] M. Nasr, S. Said, Arch. Pharmacol. 336 (2003) 551.
[26] M. Shaharyar, A. Siddiqui, M. Ali, D. Sriram, P. Yogeeswari, Bioorg. Med. Chem. Lett. 16 (2006) 3947–3949.
[27] S. Ojha, A. Bapna, G. Talesara, ARKIVOC 11 (2008) 112–122.
[28] J. Ahn, H. Kim, S. Jung, S. Kang, K. Kim, S. Rhee, S. Yang, H. Cheon, S. Kim, Bioorg. Med. Chem. Lett. 14 (2004) 4461–4465.
[29] K. Unverferth, J. Engel, N. Hofgen, A. Rostock, R. Gunther, H. Lankau, M. Menzer, A. Rolfs, J. Liebscher, B. Muller, H. Hofmann, J. Med. Chem. 41 (1998) 63–73.
[30] K.P. Bhusari, N.D. Amnerkar, P.B. Khedekar, R.D. Chakole, Indian J. Heterocycl. Chem. 15 (2005) 27–30.
[31] Phase, Version 3.0.110. Schrödinger Inc., LLC, New York, USA, 2008.
[32] S.L. Dixon, A.M. Smondyrev, E.H. Knoll, S.N. Rao, D.E. Shaw, R.A. Friesner, J. Comput. Aided Mol. Des. 20 (2006) 647–671.
[33] A. Flohr, R. Roetne, R. Norcross, C. Riemer, U. S. Patent 6,734,179 B2, 2004.
[34] J.R. Boissier, P. Simon, Arch. Int. Pharmacodyn. Ther. 158 (1965) 212–214.
[35] R.D. Porsolt, G. Anton, N. Blanet, M. Jalbre, Eur. J. Pharmacol. 47 (1978) 379–386.
[36] S. Reitman, S. Frankel, Am. J. Clin. Pathol. 28 (1957) 56–58.
[37] S. Leone, C. Mutti, A. Kazantsev, M. Sturlese, S. Moro, E. Cattanco, D. Rigamonti, A. Contini, Bioorg. Med. Chem. 16 (2008) 5695–5703.
[38] S.L. Dixon, A.M. Smondyrev, S.N. Rao, Chem. Biol. Drug Des. 67 (2006) 370–372.
[39] D.A. Evans, T.N. Doman, D.A. Thorner, M.J. Bodkin, J. Chem. Inf. Model 47 (2007) 1248–1257.
[40] Daylight chemical information systems.http://www.daylight.com (2000).